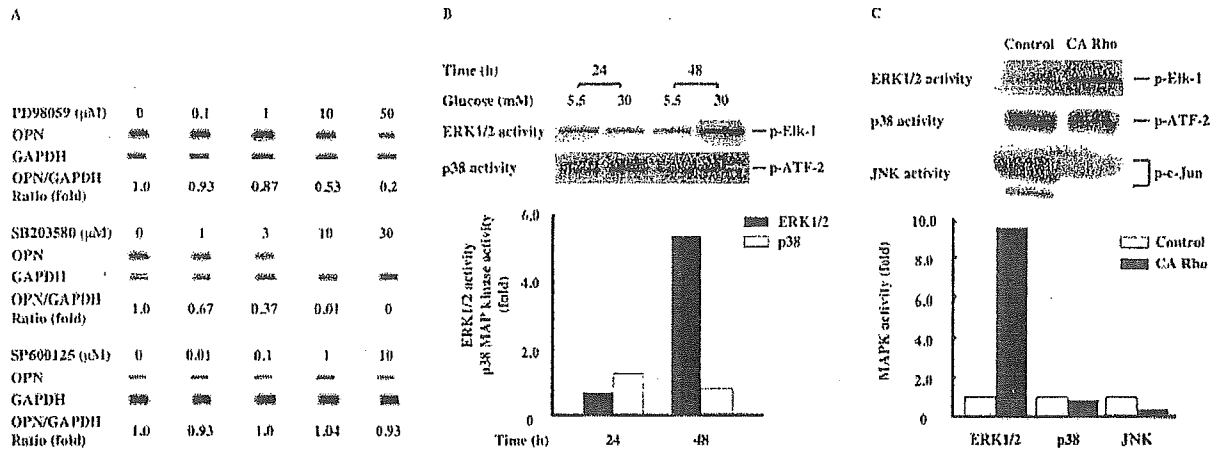

Figure 4. A, Effects of MAP kinase inhibitors on OPN expression in cultured rat aortic SMC. After serum-starvation for 24 hours, cells were incubated with the indicated concentrations of PD98059, SB203580, or SP600125 in serum-free medium containing 30 mmol/L glucose for 48 hours. After incubation, cells were processed for Northern blotting as described in the legend to Figure 1. B, High glucose-induced ERK activation in cultured rat aortic SMC. After serum-starvation for 24 hours, cells were incubated in serum-free medium containing either 5.5 mmol/L or 30 mmol/L glucose for 24 to 48 hours. After incubation, activities of ERK1/2 and p38 MAP kinase in cell lysates were measured by immune complex kinase assay with an immobilized phospho p44/42 MAP kinase antibody and Elk-1 protein as substrate, or with an immobilized phospho p38 MAP kinase antibody and ATF-2 protein as substrate, respectively. After phosphorylation reactions, samples were processed for Western blotting with phospho Elk-1 antibody or phospho ATF-2 antibody. Data are expressed as fold increase relative to the value obtained in 5.5 mmol/L glucose at the indicated times. C, Effect of transient transfection of a constitutive active Rho mutant (CA Rho) on activation of MAP kinases in cultured rat aortic SMC. Cells were transfected with 3 μg of pSRα-myc-RhoDA and incubated for 48 hours as described in the legend to Figure 2. After incubation, MAP kinase activities in cell lysates were determined. Data are expressed as fold increase relative to the value obtained in the absence of CA Rho. Double bands in the JNK activity assay correspond to 37- and 35-kilodalton forms of phosphorylated c-Jun fusion proteins. Data shown in this figure are representative of at least 2 independent experiments providing essentially similar results.

UTP-induced OPN increase and migration, demonstrating the central role of OPN in this process. The finding, together with our present observation, underscores the importance of Rho in OPN expression.

Our present finding that high glucose induces Rho activation sheds new light on the mechanism of the accelerated atherogenesis in diabetes mellitus, because involvement of Rho/Rho kinase pathway has been implicated in a wide variety of atherosclerotic processes, including neointimal formation,[15] vasospastic response,[16,17] proliferation,[18,19] migration,[19,20] and anti-apoptosis[20,21] of vascular SMC, and vascular gene expression of monocyte chemoattractant protein-1,[22] transforming growth factor-β1,[22] and inducible nitric oxide synthase.[23] Besides our present study using rat aortic SMC, high glucose-induced Rho activation was also observed in cultured rat mesangial cells[24] and in basilar artery derived from streptozotocin-induced diabetic rats.[25] It is thus conceivable that high glucose promotes diabetic vascular complications not only by upregulation of OPN but also by more diverse effects resulting from Rho activation.

It was reported that transfection of vascular SMC with the c-Ha-rasEJ oncogene induced overexpression of OPN.[26] It is well known that farnesylation is prerequisite for Ras to exert its cellular effect; therefore, our present finding that the inhibitor of farnesyltransferase, FTI-277, suppressed OPN expression might be ascribed to the inhibition of Ras function by the drug. In our previous study, however, the inhibitory effect of Pitavastatin on OPN expression in cultured rat aortic SMC was almost completely reversed by the addition of mevalonate or geranylgeranylpyrophosphate but not by farnesylpyrophosphate.[13] Studies using other types of cells, fibroblasts,[27] or keratinocytes[28] showed that transfection of dominant-negative Rho or dominant-negative Rac suppressed Ras-induced activation of Raf-MEK-ERK pathway, indicating that Ras requires either Rho or Rac function in activation of Raf-MEK-ERK pathway. Based on these findings, it is speculated that the inability of farnesylpyrophosphate to rescue the cells from the inhibition of OPN expression by Pitavastatin might be caused by suppression of Rho family function in Pitavastatin-treated cells. Further study is necessary to prove this possibility.

Acknowledgments

This work was supported by grants-in-aid 12770633, 13216018, 13204010, and 14571086; grants from the Ministry of Health, Labor, and Welfare; grants from Japan Heart Foundation; and grants from Mitsui Sumitomo Welfare Foundation, which were provided to Koutaro Yokote. Seijiro Mori received grants from the Ministry of Health, Labor, and Welfare, Comprehensive Research on Aging and Health, and Research on Specific Diseases, and from Yamanouchi Pharmaceutical Co, Ltd.

References

1. Sodek J, Ganss B, McKee MD. Osteopontin. *Crit Rev Oral Biol Med.* 2000;11:279–303.
2. Xie Y, Sakatsume M, Nishi S, Narita I, Arakawa M, Gejyo F. Expression, roles, receptors, and regulation of osteopontin in the kidney. *Kidney Int.* 2001;60:1645–1657.
3. Cantor H. The role of Eta-1/osteopontin in the pathogenesis of immunological disorders. *Ann N Y Acad Sci.* 1995;760:143–150.
4. Senger DR, Perruzzi CA, Papadopoulos A. Elevated expression of secreted phosphoprotein 1 (osteopontin, 2ar) as a consequence of neoplastic transformation. *Anticancer Res.* 1989;9:1291–1300.
5. Craig AM, Bowden GT, Chambers AF, Spearman MA, Greenberg AH, Wright JA, McLeod M, Denhardt DT. Secreted phosphoprotein mRNA is induced during multi-stage carcinogenesis in mouse skin and correlates

with the metastatic potential of murine fibroblasts. *Int J Cancer* 1990;46: 133–137.
6. Kohri K, Nomura S, Kitamura Y, Nagata T, Yoshioka K, Iguchi M, Yamate T, Umekawa T, Suzuki Y, Sinohara H, Kurita T. Structure and expression of the mRNA encoding urinary stone protein (osteopontin). *J Biol Chem.* 1993;268:15180–15184.
7. Liaw L, Birk DE, Ballas CB, Whitsitt JS, Davidson JM, Hogan BL. Altered wound healing in mice lacking a functional osteopontin gene (spp1). *J Clin Invest.* 1998;101:1468–1478.
8. Shanahan CM, Cary NR, Metcalfe JC, Weissberg PL. High expression of genes for calcification-regulating proteins in human atherosclerotic plaques. *J Clin Invest.* 1994;93:2393–2402.
9. Liaw L, Lombardi DM, Almeida MM, Schwartz SM, deBlois D, Giachelli CM. Neutralizing antibodies directed against osteopontin inhibit rat carotid neointimal thickening after endothelial denudation. *Arterioscler Thromb Vasc Biol.* 1997;17:188–193.
10. Takemoto M, Yokote K, Nishimura M, Shigematsu T, Hasegawa T, Kon S, Uede T, Matsumoto T, Saito Y, Mori S. Enhanced expression of osteopontin in human diabetic artery and analysis of its functional role in accelerated atherogenesis. *Arterioscler Thromb Vasc Biol.* 2000;20: 624–628.
11. Takemoto M, Yokote K, Yamazaki M, Ridall AL, Butler WT, Matsumoto T, Tamura K, Saito Y, Mori S. Enhanced expression of osteopontin by high glucose in cultured rat aortic smooth muscle cells. *Biochem Biophys Res Commun.* 1999;258:722–726.
12. Morisaki N, Takahashi K, Shiina R, Zenibayashi M, Otabe M, Yoshida S, Saito Y. Platelet-derived growth factor is a potent stimulator of expression of intercellular adhesion molecule-1 in human arterial smooth muscle cells. *Biochem Biophys Res Commun.* 1994;200:612–618.
13. Takemoto M, Kitahara M, Yokote K, Asaumi S, Take A, Saito Y, Mori S. NK-104, a 3-hydroxy-3-methylglutaryl coenzyme A reductase inhibitor, reduces osteopontin expression by rat aortic smooth muscle cells. *Br J Pharmacol.* 2001;133:83–88.
14. Chaulet H, Desgranges C, Renault MA, Dupuch F, Ezan G, Peiretti F, Loirand G, Pacaud P, Gadeau AP. Extracellular nucleotides induce arterial smooth muscle cell migration via osteopontin. *Circ Res.* 2001;89: 772–778.
15. Sawada N, Itoh H, Ueyama K, Yamashita J, Doi K, Chun TH, Inoue M, Masatsugu K, Saito T, Fukunaga Y, Sakaguchi S, Arai H, Ohno N, Komeda M, Nakao K. Inhibition of Rho-associated kinase results in suppression of neointimal formation of balloon-injured arteries. *Circulation.* 2000;101:2030–2033.
16. Kandabashi T, Shimokawa H, Mukai Y, Matoba T, Kunihiro I, Morikawa K, Ito M, Takahashi S, Kaibuchi K, Takeshita A. Involvement of rho-kinase in agonists-induced contractions of arteriosclerotic human arteries. *Arterioscler Thromb Vasc Biol.* 2002;22:243–248.
17. Shimokawa H, Morishige K, Miyata K, Kandabashi T, Eto Y, Ikegaki I, Asano T, Kaibuchi K, Takeshita A. Long-term inhibition of Rho-kinase induces a regression of arteriosclerotic coronary lesions in a porcine model in vivo. *Cardiovasc Res.* 2001;51:169–177.
18. Laufs U, Marra D, Node K, Liao JK. 3-Hydroxy-3-methylglutaryl-CoA reductase inhibitors attenuate vascular smooth muscle proliferation by preventing rho GTPase-induced down-regulation of p27(Kip1). *J Biol Chem.* 1999;274:21926–21931.
19. Seasholtz TM, Majumdar M, Kaplan DD, Brown JH. Rho and Rho kinase mediate thrombin-stimulated vascular smooth muscle cell DNA synthesis and migration. *Circ Res.* 1999;84:1186–1193.
20. Shibata R, Kai H, Seki Y, Kato S, Morimatsu M, Kaibuchi K, Imaizumi T. Role of Rho-Associated Kinase in Neointima Formation After Vascular Injury. *Circulation.* 2001;103:284–289.
21. Guijarro C, Blanco-Colio LM, Ortego M, Alonso C, Ortiz A, Plaza JJ, Diaz C, Hernandez G, Egido J. *Circ Res.* 1998;83:490–500.
22. Kataoka C, Egashira K, Inoue S, Takemoto M, Ni W, Koyanagi M, Kitamoto S, Usui M, Kaibuchi K, Shimokawa H, Takeshita A. Important role of Rho-kinase in the pathogenesis of cardiovascular inflammation and remodeling induced by long-term blockade of nitric oxide synthesis in rats. *Hypertension.* 2002;39:245–250.
23. Chen H, Ikeda U, Shimpo M, Ikeda M, Minota S, Shimada K. Fluvastatin upregulates inducible nitric oxide synthase expression in cytokine-stimulated vascular smooth muscle cells. *Hypertension.* 2000;36: 923–928.
24. Danesh F, Sadechi MM, Amro N, Phillips C, Zeng L, Lin S, Sahai A, Kanwar YS. 3-Hydroxy-3-methylglutaryl CoA reductase inhibitors prevent high glucose-induced proliferation of mesangial cells via modulation of Rho GTPase/p21 signaling pathway: implications for diabetic nephropathy. *Proc Natl Acad Sci USA.* 2002;99:8301–8305.
25. Miao L, Calvert JW, Tang J, Zhang JH. Upregulation of small GTPase RhoA in the basilar artery from diabetic (mellitus) rats. *Life Sci.* 2002; 71:1175–1185.
26. Parrish AR, Weber TJ, Ramos KS. Osteopontin overexpression in vascular smooth muscle cells transfected with the c-Ha-rasEJ oncogene. *In Vitro Cell Dev Biol Anim.* 1997;33:584–587.
27. Li W, Chong H, Guan KL. Function of the Rho family GTPases in Ras-stimulated Raf activation. *J. Biol Chem.* 2001;276:34728–34737.
28. Mainiero F, Murgia C, Wary KK, Curatola AM, Pepe A, Blumemberg M, Westwick JK, Der CJ, Giancotti FG. The coupling of $\alpha 6\beta 4$ integrin to Ras-MAP kinase pathways mediated by Shc controls keratinocyte proliferation. *EMBO J.* 1997;16:2365–2375.

Journal of Atherosclerosis and Thrombosis Vol. 10, No. 4

Review

Bone Marrow-derived Vascular Cells in Response to Injury

Koutaro Yokote, Ayako Take, Chiaki Nakaseko, Kazuki Kobayashi, Masaki Fujimoto, Harukiyo Kawamura, Yoshiro Maezawa, Miki Nishimura, Seijiro Mori, and Yasushi Saito

Department of Clinical Cell Biology and Medicine, Chiba University Graduate School of Medicine, Chiba, Japan.

Intimal hyperplasia is a key lesion for various vascular disorders such as atherosclerosis, postangioplasty restenosis and transplant arteriopathy. It has widely been accepted that intimal smooth muscle cells (SMC) originate from the medial layer in the same artery. However, recent studies suggest that bone marrow can also provide circulating progenitors for vascular SMC. Bone marrow-derived SMC participate in neointimal formation in animal models of allotransplantation, severe mechanical injury and hyperlipidemia-induced atherosclerosis. In human, transplantation arteriopathy also seems to involve circulating SMC, but their role in atherosclerosis and restenosis remains to be elucidated. Mobilization, differentiation and proliferation steps of SMC progenitors will provide promising targets for novel therapeutic approaches against proliferative vascular diseases. ***J Atheroscler Thromb, 2003; 10: 205–210.***

Key words: Response to injury, Smooth muscle cells, Progenitor, Bone marrow

Introduction

Neointimal hyperplasia is a common feature of various cardiovascular disease such as atherosclerosis, postangioplasty restenosis, transplant arteriopathy and pulmonary hypertension. Neointima typically consists of smooth muscle cells (SMC) and extracellularly deposited matrix. In atherosclerotic vascular lesions, the intimal structure is even more complicated by the involvement of monocyte-derived foamy macrophages and T lymphocytes which derive from blood stream (1).

Intimal and medial SMC differ from each other in several aspects, *e.g.* cytoskeletal characters, responses to growth factors/cytokines and their ability to deposit matrix. It has widely been accepted, as proposed by Russel Ross and others in the "Response to Injury" hypothesis, that the intimal SMC originate from the medial layer of the artery (2). According to their theory, vascular injury leads to endothelial dysfunction and subsequent upregulation of local growth factors and cytokines. These changes in turn prompts transition of medial contractile SMC into more synthetic phenotype, whereby they migrate into the intimal layer and proliferate.

Some groups proposed that not only SMC but other type of mesenchymal cells like adventitial fibroblasts might also be involved in formation of neointima (3, 4). More recently, bone marrow has emerged as a new source of intimal SMC or SMC-like cells (5–7). Precise understanding on the origin of neointimal SMC may provide a clue to develop an ideal therapeutical approach towards vascular diseases. We will overview the pathological significance of bone marrow-derived vascular cells with special emphasis on SMC in this review article.

Address for correspondence: Koutaro Yokote, Department of Clinical Cell Biology and Medicine, Chiba University Graduate School of Medicine, 1–8–1 Inohana, Chuo-ku, Chiba 260–8670, Japan.
E-mail: kyokote-cib@umin.ac.jp
Received February 12, 2003.
Accepted for publication February 19, 2003.

Where Do Neointimal SMC Come From?

Although extensive researches have been carried out to clarify the cause of intimal proliferative vascular disorders, the origin of intimal SMC remains controversial.

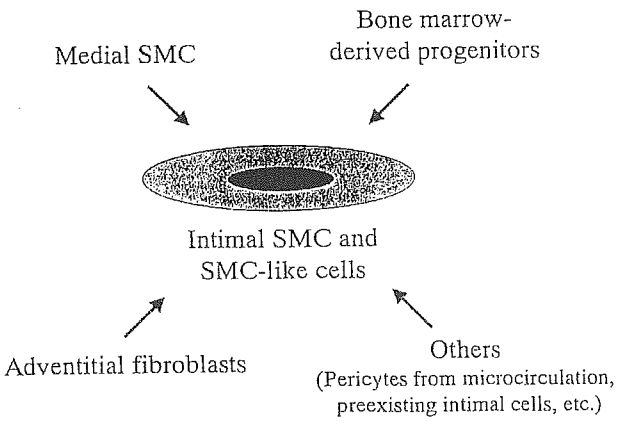

Fig. 1. Possible origin of intimal SMC and SMC-like cells. SMC; smooth muslce cells

Figure 1 shows currently presented theories concerning the source of intimal SMC. Change in medial SMC from contractile to synthetic phenotype followed by migration into the intima is so far the most widely accepted mechanism of neointimal formation (2, 8). In addition, Shi *et al.* suggested the possibility that adventitial fibroblasts migrate towards the lumen, differentiate into myofibroblasts and participate in neointimal formation (3). Other proposed cause of neointimal hyperplasia include expansion of preexisting intimal cells and circulating pericytes those derive from microvessels (3). Recently, several groups independently discovered that bone marrow-derived cells with some features of SMC accumulated in neointima in animal models of transplantation arteriopathy or severe vascular injury (5–7). It has long been believed that the only source of endothelial cells and SMC in adults is the blood vessel wall. However, since Asahara *et al.* established the concept of "circulating endothelial progenitors" which contribute to vasculogenesis in adult tissues under both physiological and pathological conditions, the bone marrow cells have been highlighted for their remarkable plasticity (9). The circulating SMC progenitors can be a new therapeutic target for various proliferative vascular diseases. On the other hand, there also are results indicating that bone marrow is unlikely to be the source of neointimal SMC (10, 11). Pathological relevance of bone marrow-derived SMC will be discussed in the further sections.

Bone Marrow-derived SMC in Response to Vascular Injury

Transplant arteriopathy

Table 1 summarizes published studies in which contribution of bone marrow as a source of intimal SMC was examined. So far, at least 4 papers have been presented by independent research groups investigating the cell origin of intimal SMC in rodent aortic allograft models (5–7, 12). According to their results, between 10 to 70% of the neointimal SMC were shown to originate from the recipient tissue. Shimizu *et al.* performed allogenic aortic transplantation from BALB/c (B/c) mice into C57BL/6 (B6) ROSA26 β-galactosidase (LacZ) transgenic mice which ubiquitously express LacZ (LacZ mice) (7). The graft after 8 weeks showed marked neointimal hyperplasia mostly composed of the cells double positive for X-gal and α-smooth muscle actin (α-SMA), which are the markers of the recipient cells and SMC, respectively. When B/c aortic transplantation was performed into irradiated wildtype B6 recipients of B6 LacZ mice-bone marrow cells, approximately 10.8% of α-SMA-expressing intimal cells also stained positive for X-gal. The results suggested that at least part of the intimal SMC-like population is accounted for by circulating bone marrow-derived cells. However, the origin of other recipient-derived SMC-like cells was not determined in the study.

Hu *et al.* also showed that the majority of intimal SMC in allogenic transplant arteriopathy and transplant atherosclerosis originates from recipients, but carefully disproved that bone marrow served as the source (11). They utilized transgenic mice expressing LacZ only in SMC (SM-LacZ). When B/c aorta was transplanted to irradiated wildtype B6 recipients of B6 SM-LacZ bone marrow, no LacZ activity was found in the graft intima indicating that the bone marrow cells were unlikely to be a source of SMC in allografts. Supported by previous reports and their own observation, they claimed that X-gal/α-SMA double positive cells observed by other groups could be artificial, since those cells might have been adjascent regions of SMC and leukocytes that were too close to be separately recognized in the sections. This is in accord with a study previously performed by Li *et al.* (10) in which they used *in situ* hybridization of sex-chromosome markers to identify the cell origin. In their study, female to male aortic allograft abundantly contained Y-chromosome-positive or recipient-derived intimal cell which co-labeled for α-SMA by immunostaining. However, in female-to-female allografts in recipients with male bone marrow showed limited number of intimal Y-chromosome positive cells, and none of these clearly co-labeled for α-SMA. The results suggested that the SMC were indeed of recipient origin, but the bone marrow was unlikely to be their source. Moreover, these cells declined in number throughout the time after transplantation consistent with graft-infiltrating inflammatory cells.

A few reports referred to pathological significance of circulating or bone marrow-derived SMC progenitors in development of organ transplant arteriopathy other than arterial grafts. Saiura *et al.* elegantly showed the involvement of bone marrow-derived α-SMA positive cells in coronary neointimal hyperplasia by performing heterotopic cardiac transplantation between the wildtype and LacZ mice (6). It is to be noted that the cells of bone

Table 1. Summary of previous studies those examined the contribution of bone marrow as a source of intimal SMC.

Experimental design	Species	Method to determine the cell origin	SMC determination	Origin of Intimal SMC	BM-derived SMC	Publication
Transplantation arteriopathy						
Aortic allotransplantation	mice	Y-Chr/ISH	SMA staining	Adjacent recipient aorta	Few if any	Li *et al.* 2001 (10)
Aortic allotransplantation with or without hyperlipidemia	mice	ROSA26 mice with X-gal staining	SMA staining	Recipient cells	10.8% of intimal SMC	Shimizu *et al.* 2001 (7)
Aortic allotransplantation	mice	ROSA26 mice with X-gal staining	SM-LacZ transgenic, X-gal staining	Recipient tissue but not from bone marrow	Not detected	Hu *et al.* 2002 (11)
Aortic allotransplantation	rat	Y-Chr/Real-time PCR	SMA staining	Recipient cells involved (70%)	Present	Religa *et al.* 2002 (12)
Cardiac allotransplantation	mice	ROSA26 mice with X-gal staining	SMA staining	Recipient cells involved (86.2%)	Majority of intimal SMC	Saiura *et al.* 2001 (6)
Cardiac allotransplantation	human	Sex-Chr/ISH	SMA staining	Recipient-derived SMC present	Present	Quaini *et al.* 2002 (18)
Renal allotransplantation	human	Y-Chr/ISH	SMA staining	Recipient cells involved (30%)	Present	Grimm *et al.* 2001 (17)
Restenosis and atherosclerosis						
Congenic BMT followed by arterial injury	mice	Y-Chr/ISH	SMA staining	Bone marrow cells involved (56%)	Majority of intimal SMC	Han *et al.* 2001 (5)
Isogenic BMT followed by arterial injury or hyperlipidemia	mice	GFP, ROSA26 with X-gal staining	SMA staining	Bone marrow cells involved (60%)	Majority of intimal SMC	Sata *et al.* 2002 (14)
Vein isograft with hyperlipidemia	mice	ROSA26 staining with X-gal staining, and Y-Chr/ISH	SM-LacZ transgenic, X-gal staining	Both donor (60%) and host (40%) cells involved, but not from bone marrow	Not detected	Hu *et al.* 2002 (16)

SMC; smooth muslce cells, SMA; α-smooth muscle action, Y-Chr; Y-chromosome, Sex-Chr; Sex-chromosome, ISH; in situ hybridization, ROSA26; transgenic ubiquitously expressing β-gal

marrow origin accounted for up to 86% of the intimal cells in their study. Vascular bed-specific differences between aorta and coronary artery may in part explain the degree of bone marrow cell contribution in the intimal hyperplasia.

Postangioplasty restenosis

Atherosclerosis and postangioplasty restenosis are other important vascular disorders also characterized by intimal hyperplasia. They affect large number of population especially in the Western countries and in Japan (13). Several research groups have investigated whether vascular smooth muscle cells might derive from bone marrow in animal models of postangioplasty restenosis.

Han *et al.* performed congenic male-to-female bone marrow transplantation followed by arterial injury, and examined localization of donor cells using Y-chromosome *in situ* hybridization in mice (5). They showed that bone marrow-derived cells are recruited in vascular healing as a complementary source of SM-like cells when the media is severely damaged and few resident SMC are available for effective repairment. Molecular mechanisms by which these cells are mobilized and led to injured vessels is yet to be discovered.

Sata *et al.* also examined whether bone marrow serves as the source for arterial SMC upon mechanical vascular injury (14). They wire-injured the femoral artery of irradiated B6 mice to which LacZ transgenic bone marrow was transplanted. The procedure resulted in neointimal hyperplasia, and more than 60% and 40% of intimal and medial cells, respectively, turned out to be LacZ positive, suggestive of the bone marrow origin. Moreover, they showed that c-Kit$^+$Sca-1$^+$Lin$^-$ hematopoietic stem cells (HSC) purified from GFP transgenic mice gave rise to α-SMA-expressing cells in the injured arteries *in vivo*. They also described that HSC differentiated into α-SMA-positive SMC-like cells by co-incubation with cultured rat SMC *in vitro*. The possibility of HSC fusion with SMC *in vitro* rather than transdifferentiation of HSC as suggested by Terada *et al.* (15) was not excluded in the study.

Endothelial progenitors are also implicated in neointimal formation in response to injury. Werner *et al.* described that bone marrow-derived endothelial progenitors participated in reendothelialization of injured carotid artery in mice. Interestingly, statin increased the circulating pool of endothelial progenitor cells and facilitated arrival of these cells to injured vessel wall. As the result, the lesion showed enhanced reendothelialization and decreased neointimal formation. Long-term fate of these cells and their interaction with SMC progenitors remain to be investigated.

Atherosclerosis

Atherosclerotic vascular lesion induced by hyperlipidemia is characterized by lipid rich plaque of foamy macrophages covered by so-called fibrous cap composed of intimal SMC and extracellular matrix. SMC content in fibrous cap is thought to be an important determinant of plaque stability. Sata *et al.* examined the aortic wall of hyperlipidemic ApoE knockout mice which bone marrow was reconstituted with the cells from either GFP or LacZ transgenic mice. Surprizingly, approximately 40 to 60% of α-SMA-positive cells in atherosclerotic plaques showed the bone marrow markers.

Hu *et al.* examined the origin of SMC in atherosclerotic plaque developed in isogenic vein graft (16). They grafted vena cava segments to carotid arteries between four types of transgenic mice, including transgenic LacZ mice, SM-LacZ mice expressing LacZ only in the vascular SMC, SM-LacZ/apoE(-/-) mice and the wild-type mice. LacZ-positive cells were observed in neointimal and atherosclerotic lesions of all vein segments grafted between LacZ transgenic and wild-type mice. Double staining for LacZ and cell nuclei revealed that about 40% of SMCs originated from hosts and 60% from the donor vessel. However, the host cells were unlikely to be of bone marrow origin since the vein graft did not contain X-gal-stained cells when transplanted to "chimeric" mice which bone marrow was reconstituted with SM-LacZ bone marrow cells.

It remains to be elucidated why the bone marrow cells contributed to SMC formation in arterial lesions but not in vein graft atherosclerosis.

Bone Marrow-derived SMC in Human Vascular Lesions

Are the bone marrow-derived progenitor cells also involved in SMC formation in human vascular disease just as described in the animal models?

It was reported that in female-to-male renal transplantation cases with the signs of chronic rejection, 34% of neointimal smooth muscle cells in the graft specimen expressed Y-chromosomomal signal, a marker for the recipient cells (17). Therefore, it was suggested that circulating mesenchymal precursor cells exist and are involved in arterial neointimal formation.

Quaini *et al.* described that in cardiac transplant from female donor to male recipient, 50% of coronary arterioles contained Y-chromosome-positive "recipient" cells (18). Among such vessels harboring recipient cells, 31 to 75% of the vascular smooth muscle cells showed Y-chromosome in their nuclei. Interestingly, the highest levels of chimerism, *i.e.* co-existence of donor and recipient cells, in the arterioles were found between 4 and 28 days of transplantation. The level of chimerism declined afterwards suggesting that the contribution of circulating precursors to vascular SMC occur most prominently in the early stage after transplantation.

In order to investigate the origin of human vascular SMC in the vessel wall, we examined the coronary artery autopsy specimens of two individuals who had undergone allogenic bone marrow transplantation (Table 2) (19). A patient was 40-year-old female who was transplanted a brother's bone marrow 10 years earlier. She had diabetes mellitus and her coronary artery showed marked dif-

Table 2. Examination of vascular SMC origin in cases of allogenic bone marrow transplantation.

Patient (bone marrow recipient)	Background disease	Donor of bone marrow stem cells	Systemic inflammation	Period after BMT	Method to determine the cell origin	SMC determination	Bono marrow replacement	Results
50 year-old female	Acute myelogenous leukemia	Brother	Absent	10 years	*in situ* hybridization for Y- and X-chromosomes	SMA staining	Successful	Intimal SMC were negative for bone marrow cell marker (Y-chromosome)
25 year-old female	Chronic EB virus infection with malignant lymphoma	Sister	Present	90 days	Immunohistochemical staining for ABO blood group antigens	SMA staining	Successful	Some medial cells expressed both SMA and donor blood group antigen

SMC; smooth muslce cells, SMA; α-smooth muscle actin, BMT; bone marrow transplantation

fuse intimal hyperplasia. Leukocytes in the arterial lumen were Y-chromosome-positive as determined by *in situ* hybridization indicating that the marrow had successfully been replaced with donor cells. However, none of the intimal SMC contained Y-chromosome-positive suggesting that intimal SMC were not of bone marrow origin in this case. On the other hand, examination of the other case, a female with chronic Epstein-Barr virus infection who died 90 days after receiving bone marrow from a sister, implied the presence of bone marrow-derive SMC-like cells. The donor blood type was A, and the recipient originally had the blood type of B. When the recipient's coronary artery was immunohistologically stained with a specific antibody against blood type A antigen, a group of cells in the medial layer showed positive signals indicating that they originated from the bone marrow. The cells at least in part showed characteristics of SMC, since they were positive for α-SMA but negative for panleukocyte antigen CD45. Pathophysiological significance of the bone marrow-derived SMC-like cells in vascular media but not in intima remains to be elucidated. Systemic inflammation caused by chronic EB infection might have caused of the appearance of bone marrow-derived SMC-like cells. Another possibility suggested by ours and Quaini's studies is that circulating SMC precursors appear in vessel wall early after transplantation or injury and fade away as the time goes by.

Conclusion

Many studies based on animal experiments indicate that a population of bone marrow-derived cells give rise to SMC or SM-like cells and contribute to blood vessel structure in various situations. Unsolved questions include the fate of bone marrow-derived SMC in long-term and whether they have a different role from media-derived SMC. Further characterization of circulating SMC progenitors and identification of the molecular signals which mobilize and recruit these cells to injured vessel may provide a new promising target for proliferative vascular diseases.

It is also interesting to know how these cells are involved in human atherosclerotic and restenotic lesions. Autopsy specimens from organ or bone marrow transplantation cases with advanced atherosclerosis, although such are rare, will be very informative in this aspect.

Acknoledgements: We thank Drs. Kenichi Harigaya and Kazuhiko Azuma for valuable advice and fruitful discussion.

Reference

(1) Ross R: Atherosclerosis – an inflammatory disease. N Engl J Med 340, 115–126, 1999

(2) Ross R: The pathogenesis of atherosclerosis: a perspective for the 1990s. Nature 362, 801–809, 1993

(3) Shi Y, O'Brien JE, Fard A, Mannion JD, Wang D, and Zalewski A: Advantial myofibroblasts contribute to neointimal formation in injured porcine coronary arteries. Circulation 94, 1655–1664, 1996

(4) Scott NA, Cipolla GD, Ross CE, Dunn B, Martin FH, Simonet L, and Wilcox JN: Identification of a potential role for the adventitia in vascular lesion formation after balloon overstretch injury of porcine coronary arteries. Circulation 93, 2178–2187, 1996

(5) Han CI, Campbell GR, and Campbell JH: Circulating bone marrow cells can contribute to neointimal formation. J Vasc Res 38, 113–119, 2001

(6) Saiura A, Sata M, Hirata Y, Nagai R, and Makuuchi M: Circulating smooth muscle progenitor cells contribute to atherosclerosis. Nat Med 7, 382–383, 2001

(7) Shimizu K, Sugiyama S, Aikawa M, Fukumoto Y, Rabkin E, Libby P, and Mitchell RN: Host bone-marrow cells are a source of donor intimal smooth-muscle-like cells in murine aortic transplant arteriopathy. Nat Med 7, 738–741, 2001

(8) Campbell GR, and Campbell JH: The phenotypes of smooth muscle expressed in human atheroma. Ann N Y Acad Sci 598, 143–158, 1990

(9) Asahara T, Murohara T, Sullivan A, Silver M, van der Zee R, Li T, Witzenbichler B, Schatteman G, and Isner JM: Isolation of putative progenitor endothelial cells for angiogenesis. Science 275, 964–967, 1997

(10) Li J, Han X, Jiang J, Zhong R, Williams GM, Pickering JG, and Chow LH: Vascular smooth muscle cells of recipient origin mediate intimal expansion after aortic allotransplantation in mice. Am J Pathol 158, 1943–1947, 2001

(11) Hu Y, Davison F, Ludewig B, Erdel M, Mayr M, Url M, Dietrich H, and Xu Q: Smooth muscle cells in transplant atherosclerotic lesions are originated from recipients, but not bone marrow progenitor cells. Circulation 106, 1834–1839, 2002

(12) Religa P, Bojakowski K, Maksymowicz M, Bojakowska M, Sirsjo A, Gaciong Z, Olszewski W, Hedin U, and Thyberg J: Smooth-muscle progenitor cells of bone marrow origin contribute to the development of neointimal thickenings in rat aortic allografts and injured rat carotid arteries. Transplantation 74, 1310–1315, 2002

(13) Koizumi J, Shimizu M, Miyamoto S, Origasa H, and Mabuchi H: Effect of pravastatin-induced LDL-cholesterol reduction on coronary heart disease and cerebrovascular disease in Japanese: Hokuriku lipid coronary heart disease study-pravastatin atherosclerosis trial (Holicos-PAT). J Atheroscler Thromb 9, 251–259, 2002

(14) Sata M, Saiura A, Kunisato A, Tojo A, Okada S,

Tokuhisa T, Hirai H, Makuuchi M, Hirata Y, and Nagai R: Hematopoietic stem cells differentiate into vascular cells that participate in the pathogenesis of atherosclerosis. Nat Med 8, 403–409, 2002

(15) Terada N, Hamazaki T, Oka M, Hoki M, Mastalerz DM, Nakano Y, Meyer EM, Morel L, Petersen BE, and Scott EW: Bone marrow cells adopt the phenotype of other cells by spontaneous cell fusion. Nature 416, 542–545, 2002

(16) Hu Y, Mayr M, Metzler B, Erdel M, Davison F, and Xu Q: Both donor and recipient origins of smooth muscle cells in vein graft atherosclerotic lesions. Circ Res 91, e13–e20, 2002

(17) Grimm PC, Nickerson P, Jeffery J, Savani RC, Gough J, McKenna RM, Stern E, and Rush DN: Neointimal and tubulointerstitial infiltration by recipient mesenchymal cells in chronic renal-allograft rejection. N Engl J Med 345, 93–97, 2001

(18) Quaini F, Urbanek K, Beltrami AP, Finato N, Beltrami CA, Nadal-Ginard B, Kajstura J, Leri A, and Anversa P: Chimerism of the transplanted heart. N Engl J Med 346, 5–15, 2002

(19) Yokote K, Take A, Kobayashi K, Fujimoto M, Kawamura H, Asaumi S, Mori S, and Saito Y: Identification of the origin of smooth muscle cells in human arteriosclerosis: A study on allogenic bone marrow transplantation recipients. The 12th International Vascular Biology Meeting, Karuizawa, Japan, May12–16, 2002

Available online at www.sciencedirect.com
SCIENCE DIRECT®
Biochemical and Biophysical Research Communications 305 (2003) 1002–1007
BBRC
www.elsevier.com/locate/ybbrc

Mice lacking Smad3 are protected against streptozotocin-induced diabetic glomerulopathy☆

Masaki Fujimoto,[a] Yoshiro Maezawa,[a] Koutaro Yokote,[a,*] Kensuke Joh,[b] Kazuki Kobayashi,[a] Harukiyo Kawamura,[a] Motonobu Nishimura,[c] Anita B. Roberts,[d] Yasushi Saito,[a] and Seijiro Mori[a]

[a] *Department of Clinical Cell Biology and Medicine, Chiba University Graduate School of Medicine, 1-8-1 Inohana, Chiba 260-8670, Japan*
[b] *Department of Pathology, Sakura National Hospital, 2-36-2 Ebaradai, Sakura, Chiba 285-8765, Japan*
[c] *Department of Internal Medicine, Sakura National Hospital, 2-36-2 Ebaradai, Sakura, Chiba 285-8765, Japan*
[d] *Laboratory of Cell Regulation and Carcinogenesis, National Cancer Institute, Bldg. 41, Room C629, 41 Library Dr., MSC 5055, Bethesda, MD 20892-5055, USA*

Received 10 April 2003

Abstract

Transforming growth factor-β (TGF-β) has been implicated in the development of diabetic glomerulopathy. In order to evaluate a role of Smad3, one of the major signaling molecules downstream of TGF-β, in the pathogenesis of diabetic glomerulopathy, Smad3-null mice were made diabetic with streptozotocin injection and analyzed 4 weeks after induction of diabetes. Electron microscopy revealed that the thickness of glomerular basement membrane (GBM) in wild-type diabetic mice was significantly higher than that in non-diabetic mice, whereas no appreciable GBM thickening was found in Smad3-null diabetic mice. Urinary albumin excretion was dramatically increased in wild-type diabetic mice, whereas Smad3-null diabetic mice did not show any overt albuminuria. Northern blotting revealed that mRNA levels of fibronectin and α3 chain of type IV collagen (α3Col4) in renal cortex of wild-type diabetic mice were approximately twice as much as those of non-diabetic mice, whereas their mRNA levels were not increased in Smad3-null diabetic mice. Real-time polymerase chain reaction (PCR) also confirmed diabetes-induced upregulation of fibronectin and α3Col4 in glomeruli of wild-type mice. Glomerular expression of TGF-β1, as assessed by real-time PCR, was enhanced to a similar degree in wild-type and smad3-null diabetic mice, indicating that the observed differences between wild-type and Smad3-null mice are not attributable to difference in the expression of TGF-β1. These data clearly demonstrate a critical role of Smad3 in the early phase of diabetic glomerulopathy. This may be due at least partly to the present findings that diabetes-induced upregulation of fibronectin and α3Col4 is dependent on Smad3 function.

Keywords: Diabetic glomerulopathy; Fibronectin; Smad3; Transforming growth factor β; Type IV collagen

Transforming growth factor-β (TGF-β) has been implicated in the development of diabetic glomerulopathy. Several reports have shown that TGF-β1 mRNA and protein are elevated in the kidneys of diabetic animals [1–4]. The ligand-binding TGF-β type II receptor is upregulated in the diabetic kidney as well [5,6]. Hyperglycemia appears to be a cause of the increased TGF-β1 and the type II receptor in the kidney because high glucose media reproduce these changes in cultured renal cells [5,7–10]. Finally, neutralization of TGF-β activity in cell culture and in diabetic animals prevented cellular and renal hypertrophy, overexpression of extracellular matrix proteins, and diabetic glomerulosclerosis, proving that the TGF-β system mediates many of the nephropathic effects of high glucose and diabetes [4,11,12].

The TGF-β signal itself is predominantly transduced by a family of transcription factors, the Smad proteins [13]. After binding the TGF-β ligand, the type II

☆ *Abbreviations:* FN, fibronectin; GBM, glomerular basement membrane; GAPDH, glyceraldehyde-3-phosphate dehydrogenase; PCR, polymerase chain reaction; STZ, streptozotocin; TGF-β, transforming growth factor-β; Col4, type IV collagen.

* Corresponding author. Fax: +81-43-226-2095.
E-mail address: kyokote-cib@umin.ac.jp (K. Yokote).

0006-291X/03/$ - see front matter © 2003 Elsevier Science (USA). All rights reserved.
doi:10.1016/S0006-291X(03)00885-4

receptor activates the type I receptor kinase, which then phosphorylates the receptor-regulated Smads (R-Smads), Smad2 and Smad3. After associating with a common-partner Smad (Co-Smad), or Smad4, the Smad complex translocates into the nucleus where it regulates the expression of target genes [13,14]. In contrast to the R-Smads and the Co-Smad, an inhibitory Smad (I-Smad), Smad7, down-regulates TGF-β signaling by inhibiting the phosphorylation of R-Smads by the type I receptor kinase [15].

At present, a precise role of individual signaling molecules downstream of TGF-β in pathogenesis of diabetic glomerulopathy has not been fully understood, because most of mice lacking the TGF-β signaling molecules were embryonic lethal. However, it was recently found that mice null for Smad3 survive into adulthood [16]. Therefore, in this study, we examined the mice to evaluate a role of Smad3 in the development of diabetic glomerulopathy.

Materials and methods

Animals and induction of diabetes. Six- to 10-week-old male $Smad3^{ex8/ex8}$ mice [16] and CL57/Bl6J mice were housed in the animal facilities, maintained on a 12-h light/12-h dark cycle, and fed standard laboratory chow. $Smad3^{ex8/ex8}$ mice were backcrossed for six generations to CL57/Bl6 mice. Mice were made diabetic with an intraperitoneal injection of streptozotocin (STZ; Sigma Chemical, St. Louis, MS, USA). Immediately after dissolving in an ice-cold citrate buffer at pH 4.6, STZ was injected at 100 mg/kg of body weight/day for 3 days. Control mice received the citrate buffer only. The first day of STZ injection was designated as Day 0. On Day 27, the mice were detained in individual metabolic cages for 24 h for urine collection. The urine volume was measured gravimetrically, and urinary albumin concentrations were determined with an enzyme-linked immunosorbent assay using a murine microalbuminuria kit (Albuwell M; Exocell, Philadelphia, PA, USA). On Day 28, after fasting for 12 h, mice were anesthetized by an intraperitoneal injection of 60 mg/kg sodium pentobarbiturate (Nembutal; Dainippon Chemicals, Tokyo, Japan) for further analyses. Plasma glucose and creatinine were assayed by standard procedures just before the mice were sacrificed.

Morphometric analysis. The kidneys were rapidly dissected out, and small pieces (approximately 1-mm cubes) of renal cortex were fixed in 0.1 M phosphate-buffered 1.2% glutaraldehyde, postfixed in 1% osmium tetroxide, and embedded in Epon 812. Ultrathin sections were cut, double-stained with uranyl acetate and lead citrate, and examined with a Hitachi (Tokyo, Japan) H-500H electron microscopy. Thickening of glomerular basement membrane (GBM) was determined as described [17]. Briefly, glomerular capillary loops were photographed by electron microscopy and printed to an original magnification of 30,000×. Twenty regions of the basement membrane were selected at random in a glomerulus and the thickness of each region was measured. Measurement was performed for a minimum of five glomeruli per mouse and all mice in each group were evaluated.

Northern blotting. The expression of mRNA in renal cortex was analyzed by Northern blotting. Total RNA was prepared using RNeasy mini kit (Qiagen, Valencia, CA, USA) according to the manufacturer's instructions. Northern hybridization was performed essentially as described [18] using a ^{32}P-labeled cDNA probe. To obtain hybridization probes specific for murine α1 and α3 chains of type IV collagen (Col4) or fibronectin (FN), total RNA derived from murine kidney was reverse transcribed and subjected to polymerase chain reaction (PCR) using the following murine primers. Sense and antisense primer sequences for α1Col4 (GenBank Accession No. J04694, 2043–3006 bp) were 5′-GCAGGAAAGGTTGTCCCACT-3′ and 5′-TTTGTCCTTTCTCTCCCTGGT-3′, for α3Col4 (GenBank Accession No. AF169387, 3127–4077 bp), 5′-GGAATGAAAGGG GAAAAAGG-3′ and 5′-TTTGGGGCCAGGGATAATT-3′, and for FN (GenBank Accession No. XM_129845, 5448–6046 bp), and 5′-AA GTGTGATCCCCATGAAGC-3′ and 5′-ATTGATCCCAGACCAA ACCA-3′, respectively. Predicted sizes of the amplified products were 964 bp for αlCol4, 951 bp for α3Col4, and 599 bp for FN. The PCR fragments were cloned into pDrive cloning vector (Qiagen) and their sequences were verified by direct sequencing. Hybridization was also performed with a ^{32}P-labeled glyceraldehyde-3-phosphate dehydrogenase (GAPDH) cDNA probe, in order to assess the amount of RNA loaded in each lane. Densitometric analyses of fluorograms and autoradiograms were performed using an imaging scanner (EPSON ES 8000) with the NIH Image 1.44 software.

Real-time PCR. The expression of mRNA in isolated glomeruli was quantified by real-time PCR. The isolation of glomeruli from mice was performed essentially as described [19] using Dynabeads. One to five microgram of RNA isolated from the glomeruli was used for cDNA synthesis. In all experiments, to avoid contamination of genomic DNA, the samples were treated with DNase before cDNA synthesis. In the reverse transcription reactions, we used a mixture containing oligo(dT) primer, $pd(T)_{12-18}$ (Amersham Biosciences, Piscataway, NJ, USA), and Ready-To-Go You-Prime First-Strand Beads (Amersham Biosciences) including buffer, dNTP, and murine reverse transcriptase. Quantitative PCR was performed using the SYBR Green PCR Master Mix (Perkin–Elmer Applied Biosystems, Foster City, CA, USA) and analyzed on an ABI PRISM 7000 Sequence Detector System (Perkin–Elmer Applied Biosystems). Primers were chosen with the assistance of the computer program Primer Express version 1.5 (Perkin–Elmer Applied Biosystems). The forward primer and reverse primer for each molecule were 5′-TGCCTCGGGAATGGAAAG-3′ and 5′-TT CCCATCGTCATAGCAGTT-3′ (FN, GenBank Accession No. XM_129845, 3594–3682 bp); 5′-CCCAGCCAGTCCATTTATAGAA T-3′ and 5′-CAGCGAAGCCAGCCAGAA-3′ (α3Col4, GenBank Accession No. AF169387, 5190–5274 bp); and 5′-GCAACATGTGG AACTCTACCAGA-3′ and 5′-GACGTCAAAAGACAGCCACTCA-3′ (TGF-β1, Gene Bank Accession No. M13177, 847–952 bp); and 5′-TGTGTCCGTCGTGGATCTGA-3′ and 5′-CCTGCTTCACCACC TTCTTGA-3′ (GAPDH, GenBank Accession No. M32599, 757–855 bp). The thermal cycling comprised an initial step at 50 °C for 2 min followed by a denaturation step at 95 °C for 10 min, 40 cycles at 95 °C for 15 s, and 40 cycles at 60 °C for 1 min. Varying lengths of oligonucleotides produce dissociation peaks at different melting temperatures. Consequently, at the end of the PCR cycles, the PCR products were analyzed using the heat dissociation protocol to confirm that one single PCR product was detected by SYBR dye. Each data point was repeated four times. Quantitative values were obtained from the threshold PCR cycle number at which the increase in signal associated with an exponential growth for PCR product starts to be detected. The relative mRNA levels in each sample were normalized to its GAPDH content.

Statistical analysis. Data are expressed as means ± SE. Student's *t* test was applied to determine the significance of differences between data for control and treated mice, with p value of less than 0.05 being taken as significant.

Results

In order to evaluate a role of Smad3 in the pathogenesis of diabetic glomerulopathy, wild-type and Smad3-null mice were made diabetic with an intraperitoneal

Table 1
Characteristics of the experimental groups of mice

	Wild-type		Smad3-null	
	Non-diabetic	Diabetic	Non-diabetic	Diabetic
Number of mice	22	21	6	6
Body weight (g)	28.3 ± 0.3	25.8 ± 0.4	20.7 ± 0.9	17.4 ± 1.4
Plasma glucose (mg/dl)	137 ± 6	275 ± 12	116 ± 16	341 ± 42
Urine volume (ml/day)	1.0 ± 0.1	16.0 ± 0.1	0.9 ± 0.2	2.2 ± 0.6
Plasma creatinine (mg/dl)	0.08 ± 0.01	0.10 ± 0.01	0.06 ± 0.00	0.07 ± 0.00

Data are expressed as means ± SE.

injection of STZ, and analyzed 4 weeks after induction of diabetes. Table 1 shows background data of the experimental groups of mice. Body weight of Smad3-null mice was obviously lower than that of wild-type mice. However, diabetes-associated reduction of body weight was similarly observed in wild-type and Smad3-null mice. Plasma glucose levels of diabetics were higher in wild-type and Smad3-null mice, and no significant difference was found between them, however, the degree of increase in urine volume of diabetics was relatively low in Smad3-null mice. Plasma creatinine level was not significantly different between each group of mice.

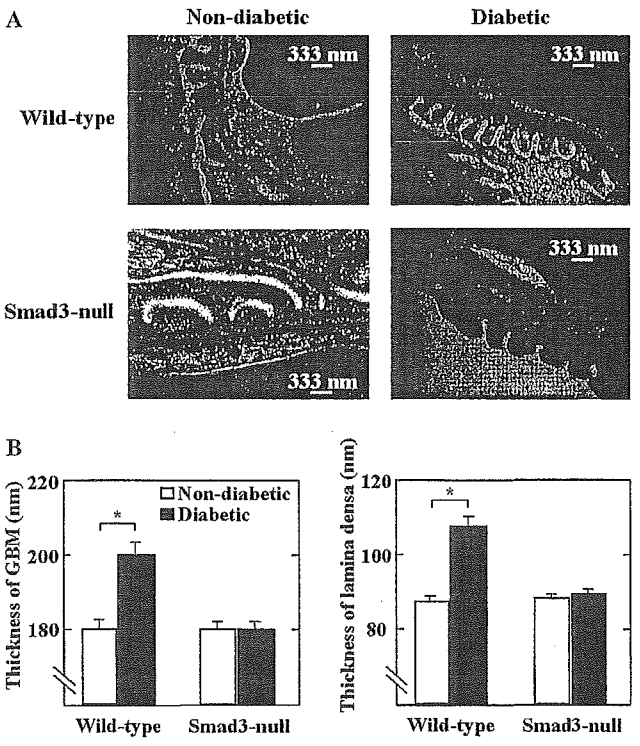

Fig. 1. (A) Electron micrographs of glomeruli in non-diabetics (left panels) and diabetics (right panels) of wild-type (upper panels) and Smad3-null (lower panels) mice (30,000×). Four weeks after induction of diabetes, the mice were anesthetized, and the kidneys were rapidly dissected out and fixed. Ultrathin sections were cut, stained, and examined with an electron microscopy. (B) Comparison of thickness of GBM and lamina densa between non-diabetics and diabetics of wild-type and Smad3-null mice. Thickness of GBM and lamina densa was determined as described in Materials and methods. Data are expressed as means ± SE ($n = 5$). *$P < 0.05$.

Fig. 1 shows electron microscopic analyses of the glomerular capillary loops of mice. In non-diabetics, there was no difference in thickness of GBM and lamina densa between wild-type and Smad3-null mice (Fig. 1A, left panels, and B). In wild-type mice, the thickness of GBM as well as lamina densa in diabetics was significantly higher than that in non-diabetics (Fig. 1A, *upper panels*, and 1B). On the other hand, in Smad3-null mice, the diabetes-associated thickening of GBM and lamina densa was not observed (Fig. 1A, *lower panels*, and 1B). Furthermore, as shown in Fig. 2, urinary albumin excretion was dramatically increased in wild-type diabetic mice, whereas Smad3-null diabetic mice did not show any overt albuminuria.

Next, we examined transcript levels of α1Col4, α3Col4, and FN in renal cortex of wild-type and Smad3-null mice by Northern blotting. As shown in Fig. 3, in wild-type mice, the expression of both FN and α3Col4 was significantly increased in diabetics as compared with that in non-diabetics, whereas no difference was found in the expression of α1Col4 between diabetics and non-diabetics. In contrast, the expression of the 3 molecules was not appreciably affected under the diabetic condition in Smad3-null mice. We further analyzed transcript levels of FN, α3Col4, and TGF-β1 in purely isolated glomeruli of wild-type and Smad3-null mice by real-time PCR. As shown in Fig. 4, the diabetes-associated up-

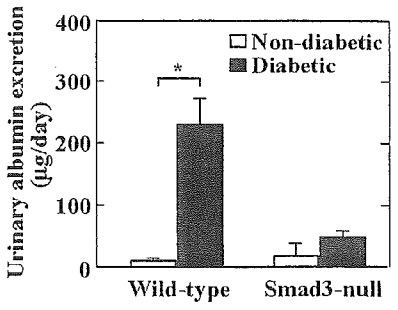

Fig. 2. Comparison of urinary albumin excretion between non-diabetics and diabetics of wild-type and Smad3-null mice. Four weeks after induction of diabetes, the mice were detained in individual metabolic cages for 24 h for urine collection. The urine volume was measured gravimetrically and urinary albumin concentrations were determined with an enzyme-linked immunosorbent assay. Data are expressed as means ± SE ($n = 5$). *$P < 0.05$.

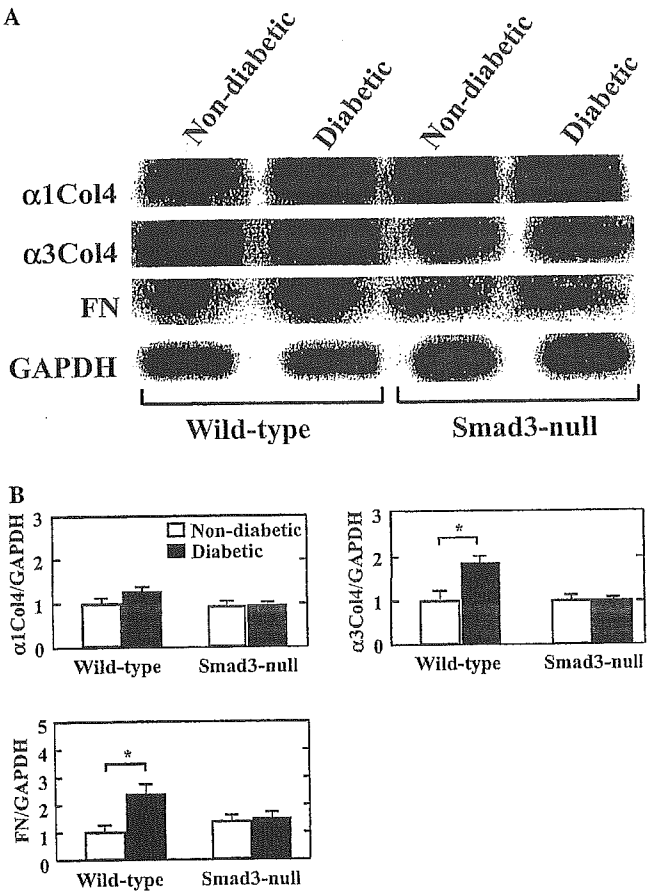

Fig. 3. Effects of diabetes on transcript levels of α1Col4, α3Col4, and FN in renal cortex of wild-type and Smad3-null mice. Four weeks after induction of diabetes, the mice were anesthetized, and the kidneys were rapidly dissected out. Total RNA was isolated from renal cortex, separated by agarose gel electrophoresis, and transferred to a nylon membrane. The membrane was hybridized with ^{32}P-labeled αlCol4, α3Col4, FN, and GAPDH cDNA probes, and signals were detected by autoradiography. (A) A representative Northern blot. (B) Comparison of transcript levels of α1Col4, α3Col4, and FN between non-diabetics and diabetics of wild-type and Smad3-null mice. The level of each transcript was estimated by the ratio of its signal to GAPDH signal on autoradiograms measured with the image analyzer. Data are expressed as means ± SE ($n = 5$). *$P < 0.05$.

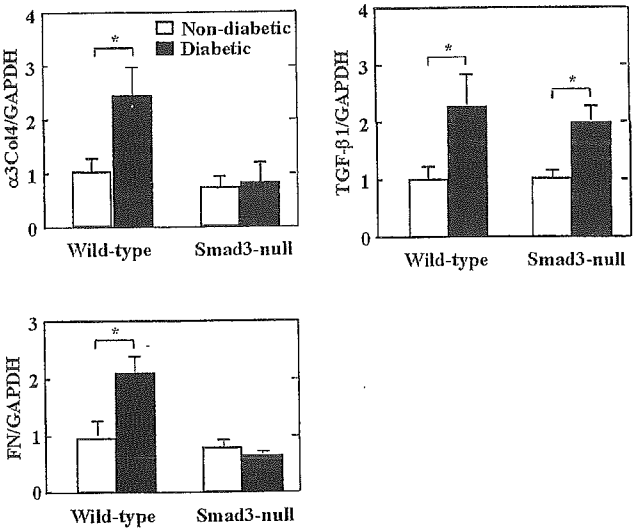

Fig. 4. Effects of diabetes on transcript levels of α3Col4, FN, and TGF-β1 in purely isolated glomeruli of wild-type and Smad3-null mice. Four weeks after induction of diabetes, the mice were anesthetized and perfused with Dynabeads through the heart. The kidneys were removed, minced, and digested with collagenase. The collagenase-digested tissue was gently pressed through a cell strainer and the suspension was then centrifuged. The pellet was resuspended and glomeruli containing Dynabeads were gathered by a magnetic particle concentrator. Then, total RNA was isolated from the isolated glomeruli and used for cDNA synthesis. Quantitative real-time PCR was performed using the SYBR Green PCR Master Mix and analyzed on an ABI PRISM 7000 Sequence Detector System. The relative mRNA levels in each sample were normalized to its GAPDH content. Data are expressed as means ± SE ($n = 5$). *$P < 0.05$.

regulation of FN as well as α3Col4 was observed also in glomeruli of wild-type mice, as expected. It was also confirmed that the expression of TGF-β1 was similarly enhanced in wild-type and Smad3-null diabetic mice.

Discussion

In the present study, analyses by electron microscopy showed that, in wild-type mice, the thickness of GBM in diabetics was significantly higher than that in non-diabetics (Fig. 1). On the other hand, in Smad3-null mice, no difference was found in the thickness of GBM between diabetics and non-diabetics (Fig. 1). Urinary albumin excretion was dramatically increased in wild-type diabetic mice, whereas Smad3-null diabetic mice did not show any overt albuminuria (Fig. 2). Northern blotting revealed that, in wild-type mice, mRNA levels of FN, a major component of both mesangial matrix and GBM [20], as well as α3Col4, a major component of GBM [21,22], in renal cortex of diabetics were approximately twice as much as those of non-diabetics (Fig. 3). In contrast, mRNA expression of FN and α3Col4 was not appreciably affected under the diabetic condition in Smad3-null mice (Fig. 3). Real-time PCR confirmed that diabetes-associated upregulation of both FN and α3Col4 was observed also in glomeruli of wild-type mice (Fig. 4). Plasma glucose levels of diabetics were similarly higher in wild-type and Smad3-null mice (Table 1) and, more importantly, glomerular expression of TGF-β1, as assessed by real-time PCR, was enhanced to a similar degree in wild-type and smad3-null diabetic mice (Fig. 4), indicating that the observed differences between wild-type and Smad3-null mice are not attributable to difference in the expression of TGF-β1. These data clearly demonstrate a critical role of Smad3 in the early phase of diabetic glomerulopathy. This may be due at least partly to the present finding that diabetes-associated upregulation of FN and α3Col4 is dependent on the existence of Smad3.

It was reported that bleomycin-induced pulmonary fibrosis [23] and radiation-induced cutaneous fibrosis [24], where enhanced TGF-β signaling seems to play an important role, were attenuated in mice lacking Smad3. In fact, Zhao et al. [23] showed that bleomycin treatment enhanced gene expression of FN and TGF-β1 in lungs of wild-type mice, and Smad3 deficiency prevented bleomycin-induced upregulation of FN without affecting TGF-β1 expression. Isono et al. [25] also have demonstrated that Smad3 mediates TGF-β-induced FN expression by using cultured rat mesangial cells transfected with dominant negative Smad3. These data are compatible with our present findings. However, studies on cultured mouse embryonic fibroblasts that were isolated from Smad3-null mice indicate that lack of Smad3 function does not block TGF-β-induced FN expression [26]. The discrepancy remains to be elucidated, but it is conceivable that dependence on Smad3 function of TGF-β-induced FN expression is variable in different cell types under different experimental conditions.

In wound healing studies of mice null for Smad3, Flanders et al. [24] have shown that loss of Smad3 interferes with the chemotaxis of inflammatory cells to TGF-β as well as their ability to autoinduce TGF-β. Based on these observations, it has been hypothesized that the reduced amount of matrix protein found in wounds in Smad3-null mice was not due to a primary effect on the fibroblasts, but rather on the reduced levels of TGF-β in the wound bed assumed to result from the markedly reduced number of macrophages and their inability to autoinduce TGF-β [27]. It is well known that most of the human and experimental glomerular diseases associated with sclerosis, including diabetic glomerulopathy [28], are characterized by the infiltration of macrophages into the glomerulus in the early stages of the disease, before the development of extracellular matrix expansion and glomerulosclerosis [29,30]. Therefore, there is a possibility that lack of diabetes-associated upregulation of FN and α3Col4 in Smad3-null mice glomeruli results from reduced glomerular infiltration of macrophages. In the present study, however, the enhanced glomerular expression of TGF-β1 was observed to a similar degree in wild-type and Smad3-null diabetic mice, suggesting that diminished response of glomerular cells to TGF-β in Smad3-deffi-cient condition accounts more for the present findings than a possible reduction of glomerular macropahge infiltration.

In summary, we have shown that loss of Smad3 gene expression attenuated diabetes-induced early glomerular changes, including thickening of GBM, albuminuria, and upregulation of FN and α3Col4 expression. Our data suggest that the local inhibition of Smad3-mediated TGF-β signal transduction may be of therapeutic benefit in prevention and treatment of diabetic glomerulopathy.

Acknowledgments

We thank Dr. Shiro Ueda for fruitful discussions and helpful suggestions. This work was supported by the following grants to Koutaro Yokote, Grant-in-Aids No. 12770633, 13216018, 13204010, and 14571086, grants from Japan Heart Foundation and Mitsui Sumitomo Welfare Foundation, and to Seijiro Mori, grants from the Ministry of Health, Labour and Welfare, and Yamanouchi Pharmaceutical Co., Ltd.

References

[1] K. Sharma, F.N. Ziyadeh, Renal hypertrophy is associated with upregulation of TGF-β1 gene expression in diabetic BB rat and NOD mouse, Am. J. Physiol. 267 (1994) F1094–F1101.
[2] T. Yamamoto, T. Nakamura, N.A. Noble, E. Ruoslahti, W.A. Border, Expression of transforming growth factor β is elevated in human and experimental diabetic nephropathy, Proc. Natl. Acad. Sci. USA 90 (1993) 1814–1818.
[3] T. Nakamura, M. Fukui, I. Ebihara, S. Osada, I. Nagaoka, Y. Tomino, H. Koide, mRNA expression of growth factors in glomeruli from diabetic rats, Diabetes 42 (1993) 450–456.
[4] K. Sharma, Y. Jin, J. Guo, F.N. Ziyadeh, Neutralization of TGF-β by anti-TGF-β antibody attenuates kidney hypertrophy and the enhanced extracellular matrix gene expression in streptozotocin-induced diabetic mice, Diabetes 45 (1996) 522–530.
[5] M. Isono, A. Mogyorosi, D.C. Han, B.B. Hoffman, F.N. Ziyadeh, Stimulation of TGF-β type II receptor by high glucose in mouse mesangial cells and in diabetic kidney, Am. J. Physiol. 278 (2000) F830–F838.
[6] S.W. Hong, M. Isono, S. Chen, M.C. Iglesias-De La Cruz, D.C. Han, F.N. Ziyadeh, Increased glomerular and tubular expression of transforming growth factor-β1, its type II receptor, and activation of the Smad signaling pathway in the db/db mouse, Am. J. Pathol. 158 (2001) 1653–1663.
[7] M.V. Rocco, Y. Chen, S. Goldfarb, F.N. Ziyadeh, Elevated glucose stimulates TGF-β gene expression and bioactivity in proximal tubule, Kidney Int. 41 (1992) 107–114.
[8] G. Wolf, K. Sharma, Y. Chen, M. Ericksen, F.N. Ziyadeh, High glucose-induced proliferation in mesangial cells is reversed by autocrine TGF-β, Kidney Int. 42 (1992) 647–656.
[9] D.C. Han, M. Isono, B.B. Hoffman, F.N. Ziyadeh, High glucose stimulates proliferation and collagen type I synthesis in renal cortical fibroblasts: mediation by autocrine activation of TGF-β, J. Am. Soc. Nephrol. 10 (1999) 1891–1899.
[10] B.L. Riser, S. Ladson-Wofford, A. Sharba, P. Cortes, K. Drake, C.J. Guerin, J. Yee, M.E. Choi, P.R. Segarini, R.G. Narins, TGF-β receptor expression and binding in rat mesangial cells: modulation by glucose and cyclic mechanical strain, Kidney Int. 56 (1999) 428–439.
[11] F.N. Ziyadeh, K. Sharma, M. Ericksen, G. Wolf, Stimulation of collagen gene expression and protein synthesis in murine mesangial cells by high glucose is mediated by autocrine activation of transforming growth factor-β, J. Clin. Invest. 93 (1994) 536–542.
[12] F.N. Ziyadeh, B.B. Hoffman, D.C. Han, M.C. Iglesias-De La Cruz, S.W. Hong, M. Isono, S. Chen, T.A. McGowan, K. Sharma, Long-term prevention of renal insufficiency, excess matrix gene expression, and glomerular mesangial matrix expansion by treatment with monoclonal antitransforming growth factor-β antibody in db/db diabetic mice, Proc. Natl. Acad. Sci. USA 97 (2000) 8015–8020.
[13] J. Massague, D. Wotton, Transcriptional control by the TGF-β/Smad signaling system, EMBO J. 19 (2000) 1745–1754.

[14] C.-H. Heldin, K. Miyazono, P. ten Dijke, TGF-β signalling from cell membrane to nucleus through SMAD proteins, Nature 390 (1997) 465–471.
[15] A. Nakao, M. Afrakhte, A. Moren, T. Nakayama, J.L. Christian, R. Heuchel, S. Itoh, M. Kawabata, N.E. Heldin, C.-H. Heldin, P. ten Dijke, Identification of Smad7, a TGF-β-inducible antagonist of TGF-β signalling, Nature 389 (1997) 631–635.
[16] G.S. Ashcroft, X. Yang, A.B. Glick, M. Weinstein, J.L. Letterio, D.E. Mizel, M. Anzano, T. Greenwell-Wild, S.M. Wahl, C. Deng, A.B. Roberts, Mice lacking Smad3 show accelerated wound healing and an impaired local inflammatory response, Nat. Cell Biol. 1 (1999) 260–266.
[17] M. Hayakawa, M. Shibata, The in vitro and in vivo inhibition of protein glycosylation and diabetic vascular basement membrane thickening by pyridoxal-5′-phosphate, J. Nutr. Sci. Vitaminol. 37 (1991) 149–159.
[18] M. Takemoto, K. Yokote, M. Yamazaki, A.L. Ridall, W.T. Butler, T. Matsumoto, K. Tamura, Y. Saito, S. Mori, Enhanced expression of osteopontin by high glucose in cultured rat aortic smooth muscle cells, Biochem. Biophys. Res. Commun. 258 (1999) 722–726.
[19] M. Takemoto, N. Asker, H. Gerhardt, A. Lundkvist, B.R. Johansson, Y. Saito, C. Betsholtz, A new method for large scale isolation of kidney glomeruli from mice, Am. J. Pathol. 161 (2002) 799–805.
[20] A. Nerlich, E. Schleicher, Immunohistochemical localization of extracellular matrix components in human diabetic glomerular lesions, Am. J. Pathol. 139 (1991) 889–899.
[21] J. Lohi, M. Korhonen, I. Leivo, L. Kangas, T. Tani, R. Kalluri, J.H. Miner, V.-P. Lehto, I. Virtanen, Expression of type IV collagen α1(IV)–α6(IV) polypeptides in normal and developing human kidney and in renal cell carcinomas and oncocytomas, Int. J. Cancer 72 (1997) 43–49.
[22] R. Kalluri, C.F. Shield, P. Todd, B.G. Hudson, E.G. Neilson, Isoform switching of type IV collagen is developmentally arrested in X-linked Alport syndrome leading to increased susceptibility of renal basement membrane to Endoproteolysis, J. Clin. Invest. 99 (1997) 2470–2478.
[23] J. Zhao, W. Shi, Y.-L. Wang, H. Chen, P. Bringas, M.B. Datto, J.P. Frederick, X.-F. Wang, D. Warburton, Smad3 deficiency attenuates bleomycin-induced pulmonary fibrosis in mice, Am. J. Physiol. Lung Cell Mol. Physiol. 282 (2002) L585–L593.
[24] K.C. Flanders, C.D. Sullivan, M. Fujii, A. Sowers, M.A. Anzano, A. Arabshahi, C. Major, C. Deng, A. Russo, J.B. Mitchell, A.B. Roberts, Mice lacking Smad3 are protected against cutaneous injury induced by ionizing radiation, Am. J. Pathol. 160 (2002) 1057–1068.
[25] M. Isono, S. Chen, S.W. Hong, M.C. Iglesias-de la Cruz, F.N. Ziyadeh, Smad pathway is activated in the diabetic mouse kidney and Smad3 mediates TGF-β-induced fibronectin in mesangial cells, Biochem. Biophys. Res. Commun. 296 (2002) 1356–1365.
[26] E. Piek, W.J. Ju, J. Heyer, D. Escalante-Alcalde, C.L. Stewart, M. Weinstein, C. Deng, R. Kucherlapati, E.P. Bottinger, A.B. Roberts, Functional characterization of transforming growth factor β signaling in Smad2- and Smad3-deficient fibroblasts, J. Biol. Chem. 276 (2001) 19945–19953.
[27] A.B. Roberts, E.P. Bottinger, G. Ashcroft, J.B. Mitchell, K.C. Flanders, Is Smad3 a major player in signal transduction pathways leading to fibrogenesis? Chest 120 (2001) S43–S47.
[28] T. Furuta, T. Saito, T. Ootaka, J. Soma, K. Obara, K. Abe, K. Yoshinaga, The role of macrophages in diabetic glomerulosclerosis, Am. J. Kidney Dis. 21 (1993) 480–485.
[29] S. Klahr, G. Schreiner, I. Ichikawa, The progression of renal disease, N. Engl. J. Med. 318 (1988) 1657–1666.
[30] B.H. Rovin, G.F. Schreiner, Cell-mediated immunity in glomerular disease, Annu. Rev. Med. 42 (1991) 25–33.

ACADEMIC PRESS

Available online at www.sciencedirect.com

SCIENCE DIRECT®

Biochemical and Biophysical Research Communications 305 (2003) 684–690

BBRC

www.elsevier.com/locate/ybbrc

Smad3 is required for enamel biomineralization

Masahiko Yokozeki,[a] Elaine Afanador,[a] Masumi Nishi,[a] Kazuyuki Kaneko,[a] Hitoyata Shimokawa,[b] Koutaro Yokote,[c] Chuxia Deng,[d] Kunihiro Tsuchida,[e] Hiromu Sugino,[e] and Keiji Moriyama[a,*]

[a] *Department of Orthodontics, School of Dentistry, The University of Tokushima, 3-18-15 Kuramoto-cho, Tokushima 770-8504, Japan*
[b] *Pharmacology, Department of Hard Tissue Engineering, Division of Bio-Matrix, Graduate School, Tokyo Medical and Dental University, 1-5-45 Yushima, Bunkyo-Ku, Tokyo 113-8549, Japan*
[c] *Second Department of Internal Medicine, School of Medicine, Chiba University, 1-8-1 Inohana, Chiba 260-0856, Japan*
[d] *Genetics of Development and Disease Branch, NIDDK, National Institute of Health, 10/9N105, 10 Center Drive, Bethesda, MD 20892, USA*
[e] *Institute for Enzyme Research, The University of Tokushima, 3-18-15 Kuramoto-cho, Tokushima 770-8503, Japan*

Received 10 April 2003

Abstract

Smad3 is an intracellular signaling molecule that mediates the signal from transforming growth factor-β (TGF-β) and activin receptors. In this study, we reveal hypomineralized enamel in mice with the targeted deletion of the Smad3 gene. The Smad3 (−/−) mice had chalky white incisor enamel, while the enamel of the wild-type or Smad3 (+/−) mice was yellow-brown. Histological analysis of the undecalcified sections showed that the enamel thickness of the maxillary incisors in the Smad3 (−/−) mice was similar to that of the wild-type and Smad3 (+/−) mice while that the enamel of the maxillary molars in Smad3 (−/−) mice was disrupted in places. Microcomputed tomography (μCT) analysis revealed that the mineralization of the maxillary incisors and mandibular molars in the Smad3 (−/−) mice showed significant reduction in the degree of mineralization when compared to that of the wild-type and Smad3 (+/−) mice. Scanning electron microscopic (SEM) analysis of the mandibular incisors revealed that the enamel surface of the Smad3 (−/−) mice was irregular and disrupted in places and showed images similar to decalcified mature enamel. The histological analysis of the decalcified sections showed that distinct morphological changes in the ameloblasts at the secretory and maturational stages were not observed between the Smad3 (−/−) and Smad3 (+/−) or wild-type mice, while the enamel matrix was observed in the decalcified sections of the mandibular molars in the Smad3 (−/−) mice. These results suggested that Smad3 was required for enamel biomineralization, and TGF-β and activin signaling might be critical for its process.

Keywords: Smad3; Enamel; Hypomineralization; Tooth development

Dental enamel, which covers the crown of a tooth, is the most highly mineralized tissue in the body. Enamel is neither replaceable nor reparable because the ameloblast that synthesizes the enamel matrix is lost at tooth eruption. Enamel is unique among hard tissues because of its high mineral content. Other hard tissues, such as bone and cartilage, consist of approximately 20–30% organic materials by weight while mature enamel contains less than 1% organic materials [1]. Although enamel matrix proteins are present during the enamel formation, these proteins are completely removed once the enamel attains its final hardened form. Therefore, the process of enamel mineralization is also unique when compared with the general biomineralization of hard tissues.

Dental enamel development consists of several stages that include the secretory, transition, and maturation stages. During the secretory stage, culomular-shaped ameloblasts, which were located adjacent to the forming enamel, secrete enamel matrix proteins. These proteins include amelogenin, ameloblastin, and enamelin [2]. The most abundant matrix protein is amelogenin that comprises about 90% of the total matrix protein of immature enamel and ameloblastin and enamelin account for

* Corresponding author. Fax: +81-88-633-9138.
E-mail address: moriyama@dent.tokushima-u.ac.jp (K. Moriyama).

0006-291X/03/$ - see front matter © 2003 Elsevier Science (USA). All rights reserved.
doi:10.1016/S0006-291X(03)00806-4

about 5% and 2%, respectively [2]. Enamelysin, which is matrix metalloproteinase-20 (MMP-20), also has important roles as an enamel matrix-processing enzyme during the secretory stage. The expression of enamelysin initiates prior to the onset of dentin mineralization and continues throughout the secretory stage in vivo, and in vitro enamelysin catalyzes the amelogenin cleavages that are known to occur during the secretory stage [2]. At the end of the secretory stage, the transition stage begins and ameloblasts shrink in size and downregulate protein release into the enamel matrix. The transition stage is followed by the maturation stage, where the enamelysin expression is eliminated [2]. The ameloblasts abruptly begin the expression of the enamel matrix serine protease 1 (EMSP1) that was officially designated as kallikrein 4 (KLK4) in the transition stage [2]. KLK4 could degrade enamel proteins during the transition and maturation stages [2]. Because enamel hardening is dependent upon the removal of enamel proteins during the maturation stage, KLK4 may play critical roles in this process. Thus, enamel proteinases play two important roles, the processing and degradation of enamel proteins, during enamel formation.

Members of the transforming growth factor-β (TGF-β) family transduce signals through type I and type II serine/threonine kinase receptors [3]. The type I receptor is a substrate for the type II receptor and propagates the signal downstream upon activation [3]. Smads, which are 50–70 kDa intracellular proteins, mediate the downstream intracellular signaling from the TGF-β family receptors to the nucleus. Receptor-regulated Smads consist of Smads2 and 3 that mediate the TGF-β and activin signaling, and Smads1, 5, and 8 mediate the BMP signaling [4]. A phosphorylated receptor-regulated Smad heterodimerizes with Smad4 and this complex translocates to the nucleus to the transactivate specific target gene [4]. Inhibitory Smads, which consist of Smads6 and 7, disrupt the signal transduction by preventing phosphorylation of the pathway-specific Smads [4].

Here we show abnormal enamel development in Smad3 mutant mice. Our observation indicated that Smad3 mutant mice had hypomineralized enamel, suggesting that Smad3 is required for the process of maturation during enamel formation.

Materials and methods

Experimental animals. The mice were maintained and used in accordance with the experimental protocols approved by the Ethical Committee of the University of Tokushima. Smad3 deficient mice were created by homologous recombination to delete exon8 of Smad3 in a previous study [5]. Mated pairs of mice heterozygous for the targeted deletion of Smad3 of a mixed 129/C57B6 background produced litters for this study. Six-week postnatal mice were used in this study. The genotype of the Smad3 mutant mice was determined by PCR as previously described [5].

Preparation of tissue sections and histological analysis. The undecalcified sections were obtained from the site of the maxillary incisors and molars. The specimens were embedded in methylmethacrylate (MMA) without staining to yield a 30-μm thick crosscut ground section, cut with a Saw Microtome (LEICA,SP1600), and stained with toluidine blue. The undecalcified sections were obtained from the site of the mandibular incisors and molars. Whole mandibles from the wild-type, heterozygous, and homozygous mice were dissected and fixed in 4% freshly made paraformaldehyde in 100 mM sodium phosphate buffer (PB, pH 7.0) for 48 h at 4 °C. The samples were then decalcified with 20% EDTA in 100 mM PB for 14 days, dehydrated, and embedded in paraffin. The tissue blocks were cut into 4-μm thick mesio-distal serial sections and mounted on 3-(triethoxylosilyl)-propylamine-coated (Merck, Schucardt, München, Germany) glass slides. They were then processed for histology.

Microcomputed tomography analysis. The mandibular molars and maxillary incisors were scanned with a micro-CT scanner (MIF-100, HITACH Medical) producing 202 10-μm thick scans. Three-dimensional images were reconstructed using TRI/3D-BON software (RATOC System Engineering, Tokyo).

Scanning electron microscope. The dissected half mandibles were ultrasonically cleaned in distilled H_2O for 10 min, air-dried, and vacuum coated with a layer of gold. The mandibular incisors and molars were examined using a scanning electron microscope (SEM) operating at 20 kV.

Results

Gross examination revealed that the Smad3 (−/−) mice dentition appeared to be morphologically normal, whereas the incisor enamel consistently lacked pigmentation, had a chalky white appearance, and was frequently broken (Fig. 1). The incisors of the wild-type and Smad3 (+/−) mice were always yellow (Fig. 1). Therefore, the Smad3 (−/−) mice could be distinguished from either the wild-type or Smad3 (+/−) mice with 100% accuracy based solely on the incisor color. It has been reported that a number of transgenic animals, which had chalky white incisors, revealed enamel defects [6–8] which suggested that the Smad3 (−/−) mice might also have enamel defects. The undecalcified sections of the maxillary incisors and molars showed that the molar enamel of the Smad3 (−/−) mice (Figs. 2c and d) was disrupted in places but not that of the wild-type and Smad3 (+/−) mice (Figs. 2a and b), and that the thickness of the incisor enamel in the Smad3 (−/−) mice was similar to that of the wild-type (Figs. 2e and f). Because only the labial side is covered by enamel in rodent incisors, the maxillary incisor enamel of the Smad3 (−/−) mice was free from mechanical force caused by mastification and the enamel might be intact in the absence of the disruption as observed in the maxillary molar enamels. Therefore, these results suggested that the phenotypic changes in the enamel of the Smad3 (−/−) mice appeared to be due to hypomineralization but not hypoplasticity. Therefore, we performed a microcomputed tomography (μCT) analysis to clarify the defects of mineralization in the Smad3 (−/−) mice. The enamel of the mandibular molars and maxillary incisors in the

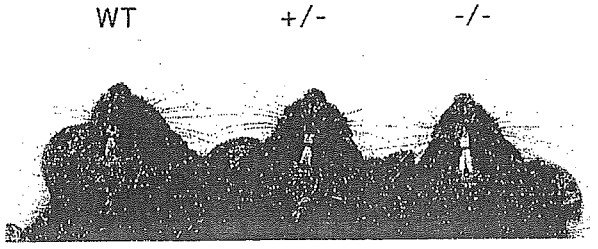

Fig. 1. Incisors in wild-type (WT), Smad3 (+/−), and Smad3 (−/−) mice. The Smad3 (−/−) incisors are always chalky white and fragile; in the present individual, the mandibular right incisor is broken. The WT and Smad3 (+/−) incisors are yellow brown.

Smad3 (−/−) mice showed a significant reduction in the degree of mineralization as compared with that of the wild-type and Smad3 (+/−) mice (Fig. 3). Examination of the mandibular incisors and molars by SEM revealed that the morphology of the incisors and molars in the Smad3 (−/−) mice was different from that of the wild-type and Smad3 (+/−) mice and its surfaces were not smooth in places (Figs. 4a–c, h, i). The high magnification of the SEM images revealed that the enamel surfaces of the Smad3 (−/−) mice were irregular when compared with the Smad3 (+/−) mice, and enamel rod and interrod structures were observed in the disrupted area even without any treatment of etching agents (Figs. 4d–g, j, k). These images were typical features of the rodent enamel by acid treatment [9,10]. The histological analysis of the decalcified sections showed that distinct morphological changes in the ameloblasts of the secretory and maturational stages were not observed between the Smad3 (−/−) and Smad3 (+/−) or wild-type mice

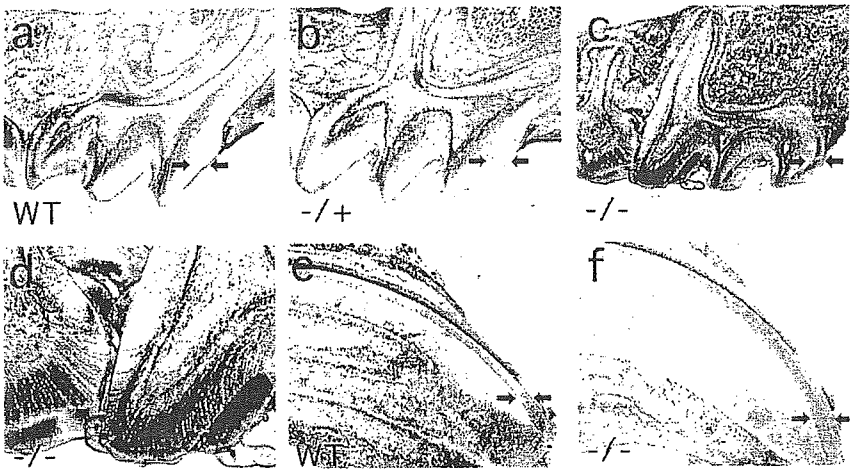

Fig. 2. Histological analysis of undecalcified sections from wild-type (a, e), Smad3 (+/−) (b) and Smad3 (−/−) (c, d, f) mice. The enamel of the maxillary first molars from the Smad3 (−/−) mice showed abnormal stainings and disrupted in places when compared to that of the wild-type and Smad3 (+/−) mice (a–d). The enamel thickness of the maxillary incisors from the Smad3 (−/−) mice was similar to that of the wild-type mice (e, f). Paired arrows indicate thickness of the enamel layer. Original magnifications: 40× (a–c, e, f), 100× (d).

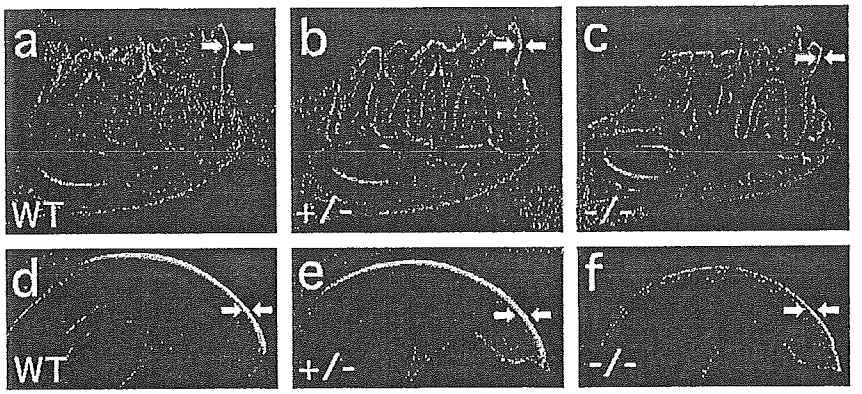

Fig. 3. μCT analysis of mandibular molars (a–c) and maxillary incisors (d–f). The enamel of the mandibular molars and maxillary incisors in Smad3 (−/−) mice (c, f) showed significant reduction in the degree of mineralization as compared with that of the wild-type (a, d) and Smad3 (+/−) mice (b, e). Paired arrows indicate thickness of the enamel layer.

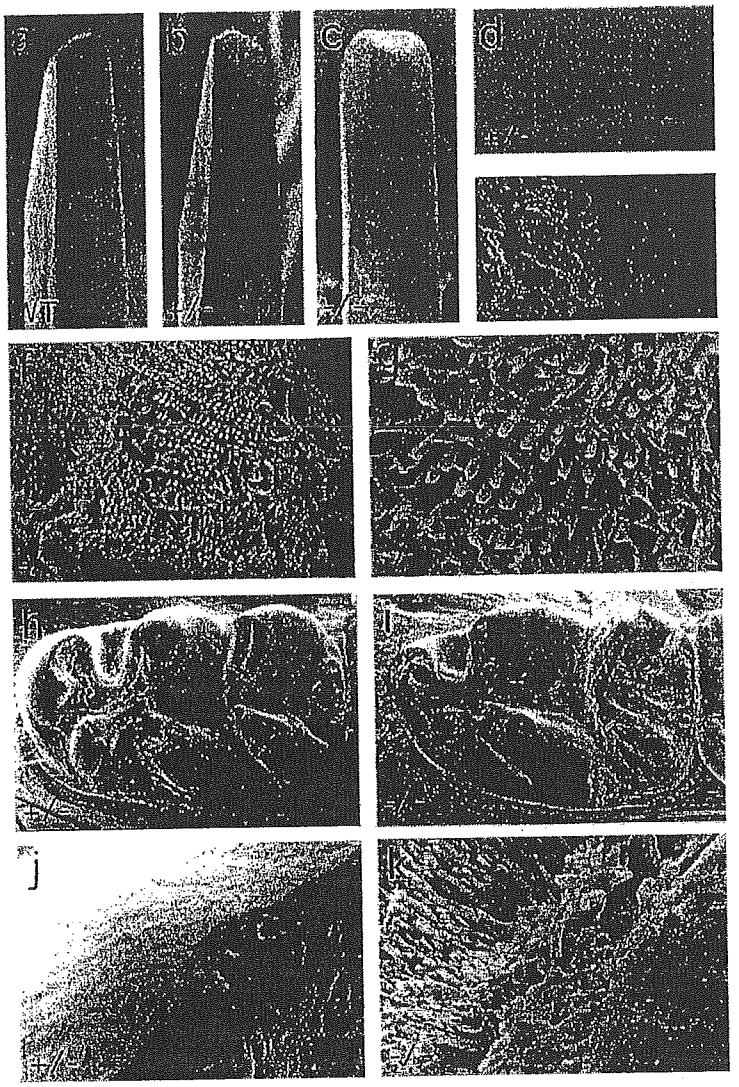

Fig. 4. SEM images of the enamel from the wild-type (a), Smad3 (+/–) (b, d, h, j), and Smad3 (–/–) (c, e, f, g, i, k) mice. The enamel from the mandibular incisors (a–g) and first molars (h–k) was observed by SEM. The mandibular incisors and molars from the wild-type and Smad3 (+/–) mice have sharp tips and smooth enamel surfaces (a, b, d) and the incisors of the Smad3 (–/–) mice have blunted tips and irregular and disrupted enamel surfaces (c, e, f, g, i, k). The molars from the Smad3 (+/–) mice have smooth enamel surfaces (h, j) and the molars from the Smad3 (–/–) mice have irregular and disrupted enamel surfaces (i, k). The SEM images were photographed at 50× (a–c), 75× (h, i), 500× (f), 1000× (d, e, j, k), and 2000× (g) magnifications.

(Figs. 5a–e). In the Smad3 (–/–) mice, the ameloblasts at the secretory stage were well formed and arranged in an orderly fashion (Fig. 5e) and these morphological features were typical as observed in the wild-type mice (Fig. 5d). In the Smad3 (–/–) mice, the ameloblasts at the maturation stage became shortened (Fig. 5c) as observed in the wild-type (Fig. 5a) or the Smad3 (+/–) mice (Fig. 5b), but the staining pattern of the enamel matrix beneath the ameloblasts of the Smad3 (–/–) mice (Fig. 5c) was stronger than that of the wild-type (Fig. 5a) or the Smad3 (+/–) mice (Fig. 5b). Interestingly, a possible enamel matrix was observed in the decalcified sections of the mandibular molars in the Smad3 (–/–) mice (Fig. 5f).

Discussion

Our phenotypic analysis of the molars and incisors in mice lacking the Smad3 gene showed hypomineralization of the enamel, but not hypoplasticity. The organic matrix appeared to be present in the mature enamel of the Smad3-deficient mice as observed in the decalcified sections of the mandibular molars. Although we examined only the enamel in this study, there were a number of studies about the phenotypic expression caused by the loss of Smad3 in the mice. The loss of the Smad3 function results in a diminished T cell response to TGF-β [5,11], accelerated wound healing [12], and colon

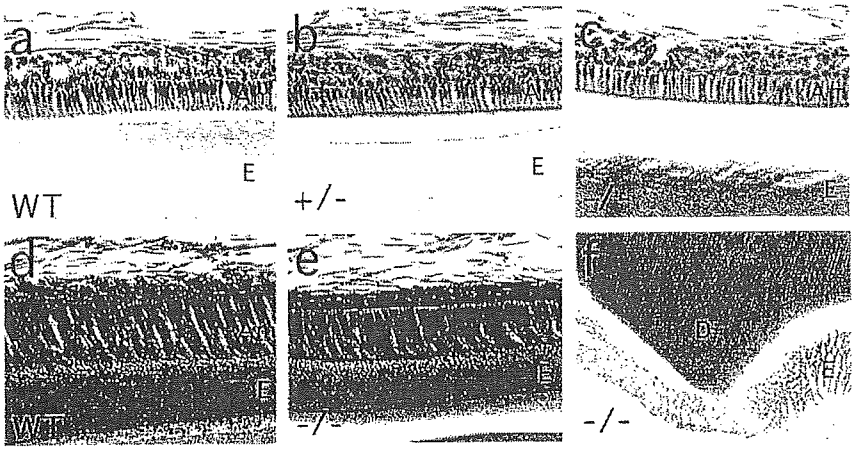

Fig. 5. Histological analysis of decalcified sections from the wild-type (a, d), Smad3 (+/−) (b), and Smad3 (−/−) (c, e, f) mice. The decalcified sections of the mandibular incisors (a–e) and molars (f) were stained with hematoxylin and eosin. Distinct morphological changes in the ameloblasts of secretory (d, e) and maturational (a–c) stages were not observed between the Smad3 (−/−) and Smad3 (+/−) or wild-type mice. The enamel matrix was observed in the mandibular molars in the Smad3 (−/−) mice (f). E, enamel; D, dentine; and Am, ameloblasts. Original magnifications: 200× (a–e) 100× (f).

cancer [13]. Furthermore, the repression of chondrocyte hypertrophic differentiation and dysregulation of osteoblast differentiation and apoptosis were observed in mice lacking the Smad3 gene and these abnormalities could lead to osteoarthritis and osteopenia, respectively [14,15]. As shown in the undecalcified sections and μCT analysis of this study, the bone mass appeared to decrease in the interradicular septum of the maxillary and mandibular first molars and the dentin thickness might be thin in the Smad3 (−/−) mice as compared with the wild-type or Smad3 (+/−) mice (Figs. 2 and 3). Therefore, in addition to the impairment of enamel mineralization in the Smad3 (−/−) mice, the loss of Smad3 might also affect the mineralization of other hard tissues.

Amelogenesis imperfecta (AI) is a common group of inherited defects of dental enamel formation that exhibit marked genetic and clinical heterogeneity with at least 14 different sub-types being recognized on the basis of their clinical appearance in humans [16]. Affected individuals show either hypoplastic or hypomineralized enamel, but an overlap of these signs is seen in many cases [17]. The enamel abnormalities in the Smad3 (−/−) mice might be similar in some aspects to the human AI conditions. The mutations in the gene encoding amelogenin and enamelin have been shown to cause some X-linked recessive and autosomal dominant forms of amelogenesis imperfecta [18–21]. Although it is unclear whether Smad3 could regulate these gene expressions, the Smad3-deficient mice might be useful animal models to elucidate the intracellular signaling molecules that play an important role in the enamel development.

Several transgenic animals have been reported as having abnormal enamel. Interestingly, TGF-β1 deficient mice revealed excessive wear of the occlusal surfaces of teeth possibly with hypomineralization of the enamel and dentine, independent of the process of inflammation [22]. Furthermore, transgenic mice that overexpress Smad2 in the epidermis under the control of the keratin 14 promoter showed abnormal enamel [23]. Mice mutated with the cystic fibrosis transmembrane regulator (CFTR) gene, which causes cystic fibrosis, had enamel with crystallite defects, retained protein, and hypomineralization [6,24]. Interestingly, epithelial cells in the CFTR mutant mice showed reduced expression of the Smad3 protein [25]. Therefore, although it is not clear whether enamel defects of these mice were identical to those of the Smad3 deficient mice, TGF-β and activin signaling through Smad3 seems to be important during enamel biomineralization.

Smad3 shares more than a 95% homology with Smad2, and Smads2 and 3 mediate TGF-β and activin signaling as receptor-regulated Smads [26]. The expressions of Smad2 and Smad3 are present in epithelially derived ameloblasts and cranial neural crest-derived odontoblasts [27,28]. Interestingly, mice lacking the Smad2 gene are early embryonic lethal [29–32], whereas Smad2 heterozygous mice showed patterning defects in which the incisors and mandibular molars fail to develop but maxillary molars normally develop, as observed in the activinβA and activin type II receptor mutant mice [33]. Furthermore, it has also been reported that Smad2, but not Smad3, played an important regulatory role in TGF-β signaling during early tooth development [34]. Thus, Smad2 might have critical roles during early tooth development. On the contrary, the enamel of the Smad3 (−/−) mice appeared to have a normal enamel thickness, and normal enamel rod and interrod structures. Thus, the secretory stage of development and secretary function of the ameloblasts in Smad3 (−/−) mice appeared to be normal and the

abnormality of the proteinases, which could degrade enamel matrix proteins, might cause the hypominaralized enamel in Smad3 (−/−) mice. Because enamelysin is the enamel matrix processing proteinase and its expression was limited in the secretory and transition stage [2], enamel abnormality as shown in this study might be independent of enamelysin. A recent study showed that the loss of enamelysin resulted in the altered enamel matrix and rod pattern and hypoplastic enamel [35] and these phenotypes were different from those of the Smad3 (−/−) mice. Because KLK4 is the enamel matrix degrading proteinase in the transition and maturation stages [2], Smad3 might have possible roles in the KLK4 expression or its function. The loss of KLK4 in mice would give us useful information about the mechanism of enamel biomineralization. Although the target molecule of Smad3 is unclear in the present study, a further analysis would be needed in order to clarify the signaling cascade through Smad3 during enamel biomineralization.

Acknowledgments

We thank H. Murayama (Kureha Chemical Industry) for the histological analysis of the undecalcified sections. This work was supported in part by the Grants-in-Aid for Scientific Research from the Japanese Ministry of Education, Nos. 13470452 and 13771263.

References

[1] J.D. Bartlett, J.P. Simmer, Proteinases in developing dental enamel, Crit. Rev. Oral Biol. Med. 10 (4) (1999) 425–441.
[2] J.P. Simmer, J.C. Hu, Expression, structure, and function of enamel proteinases, Connect. Tissue Res. 43 (2–3) (2002) 441–449.
[3] J. Massague, TGF-β signal transduction, Annu. Rev. Biochem. 67 (1998) 753–791.
[4] P. Ten Dijke, M.J. Goumans, F. Itoh, S. Itoh, Regulation of cell proliferation by Smad proteins, J. Cell Physiol. 191 (1) (2002) 1–16.
[5] X. Yang, J.J. Letterio, R.J. Lechleider, L. Chen, R. Hayman, H. Gu, A.B. Roberts, C. Deng, Targeted disruption of SMAD3 results in impaired mucosal immunity and diminished T cell responsiveness to TGF-β, EMBO J. 18 (5) (1999) 1280–1291.
[6] J.T. Wright, C.L. Kiefer, K.I. Hall, B.R. Grubb, Abnormal enamel development in a cystic fibrosis transgenic mouse model, J. Dent. Res. 75 (4) (1996) 966–973.
[7] H.M. Zhou, A. Nichols, A. Wohlwend, I. Bolon, J.D. Vassalli, Extracellular proteolysis alters tooth development in transgenic mice expressing urokinase-type plasminogen activator in the enamel organ, Development 126 (5) (1999) 903–912.
[8] C.W. Gibson, Z.A. Yuan, B. Hall, G. Longenecker, E. Chen, T. Thyagarajan, T. Sreenath, J.T. Wright, S. Decker, R. Piddington, G. Harrison, A.B. Kulkarni, Amelogenin-deficient mice display an amelogenesis imperfecta phenotype, J. Biol. Chem. 276 (34) (2001) 31871–31875.
[9] S.P. Lyngstadaas, S. Risnes, B.S. Sproat, P.S. Thrane, H.P. Prydz, A synthetic, chemically modified ribozyme eliminates amelogenin, the major translation product in developing mouse enamel in vivo, EMBO J. 14 (21) (1995) 5224–5229.
[10] M.L. Paine, D.H. Zhu, W. Luo, P. Bringas Jr., M. Goldberg, S.N. White, Y.P. Lei, M. Sarikaya, H.K. Fong, M.L. Snead, Enamel biomineralization defects result from alterations to amelogenin self-assembly, J. Struct. Biol. 132 (3) (2000) 191–200.
[11] M.B. Datto, J.P. Frederick, L. Pan, A.J. Borton, Y. Zhuang, X.F. Wang, Targeted disruption of Smad3 reveals an essential role in transforming growth factor β-mediated signal transduction, Mol. Cell Biol. 19 (4) (1999) 2495–2504.
[12] G.S. Ashcroft, X. Yang, A.B. Glick, M. Weinstein, J.L. Letterio, D.E. Mizel, M. Anzano, T. Greenwell-Wild, S.M. Wahl, C. Deng, A.B. Roberts, Mice lacking Smad3 show accelerated wound healing and an impaired local inflammatory response, Nat. Cell Biol. 1 (5) (1999) 260–266.
[13] Y. Zhu, J.A. Richardson, L.F. Parada, J.M. Graff, Smad3 mutant mice develop metastatic colorectal cancer, Cell 94 (6) (1998) 703–714.
[14] X. Yang, L. Chen, X. Xu, C. Li, C. Huang, C.X. Deng, TGF-β/Smad3 signals repress chondrocyte hypertrophic differentiation and are required for maintaining articular cartilage, J. Cell Biol. 153 (1) (2001) 35–46.
[15] A.J. Borton, J.P. Frederick, M.B. Datto, X.F. Wang, R.S. Weinstein, The loss of Smad3 results in a lower rate of bone formation and osteopenia through dysregulation of osteoblast differentiation and apoptosis, J. Bone Miner. Res. 16 (10) (2001) 1754–1764.
[16] C.J. Witkop Jr., Amelogenesis imperfecta, dentinogenesis imperfecta and dentin dysplasia revisited: problems in classification, J. Oral Pathol. 17 (9–10) (1988) 547–553.
[17] B. Backman, Amelogenesis imperfecta–clinical manifestations in 51 families in a northern Swedish county, Scand. J. Dent. Res. 96 (1988) 505–516.
[18] M.J. Aldred, P.J. Crawford, E. Roberts, N.S. Thomas, Identification of a nonsense mutation in the amelogenin gene (AMELX) in a family with X-linked amelogenesis imperfecta (AIH1), Hum. Genet. 90 (1992) 413–416.
[19] N.J. Lench, A.H. Brook, G.B. Winter, SSCP detection of a nonsense mutation in exon 5 of the amelogenin gene (AMGX) causing X-linked amelogenesis imperfecta (AIH1), Hum. Mol. Genet. 3 (1994) 827–828.
[20] M.H. Rajpar, K. Harley, C. Laing, R.M. Davies, M.J. Dixon, Mutation of the gene encoding the enamel-specific protein, enamelin, causes autosomal-dominant amelogenesis imperfecta, Hum. Mol. Genet. 10 (2001) 1673–1677.
[21] C.K. Mardh, B. Backman, G. Holmgren, J.C. Hu, J.P. Simmer, K. Forsman-Semb, A nonsense mutation in the enamelin gene causes local hypoplastic autosomal dominant amelogenesis imperfecta (AIH2), Hum. Mol. Genet. 11 (2002) 1069–1074.
[22] R.N. D'Souza, A. Cavender, D. Dickinson, A. Roberts, J. Letterio, TGF-β1 is essential for the homeostasis of the dentin–pulp complex, Eur. J. Oral. Sci. 106 (Suppl. 1) (1998) 185–191.
[23] Y. Ito, P. Sarkar, Q. Mi, N. Wu, P. Bringas Jr., Y. Liu, S. Reddy, R. Maxson, C. Deng, Y. Chai, Overexpression of Smad2 reveals its concerted action with Smad4 in regulating TGF-β-mediated epidermal homeostasis, Dev. Biol. 236 (2001) 181–194.
[24] C.K. Arquitt, C. Boyd, J.T. Wright, Cystic fibrosis transmembrane regulator gene (CFTR) is associated with abnormal enamel formation, J. Dent. Res. 81 (2002) 492–496.
[25] T.J. Kelley, H.L. Elmer, D.A. Corey, Reduced Smad3 protein expression and altered transforming growth factor- β1-mediated signaling in cystic fibrosis epithelial cells, Am. J. Respir. Cell Mol. Biol. 25 (2001) 732–738.
[26] P. ten Dijke, K. Miyazono, C.H. Heldin, Signaling via hetero-oligomeric complexes of type I and type II serine/threonine kinase receptors, Curr. Opin. Cell Biol. 8 (2) (1996) 139–145.
[27] A. Dick, W. Risau, H. Drexler, Expression of Smad1 and Smad2 during embryogenesis suggests a role in organ development, Dev. Dyn. 211 (1998) 293–305.
[28] K.C. Flanders, E.S. Kim, A.B. Roberts, Immunohistochemical expression of Smads 1–6 in the 15-day gestation mouse embryo: